

Efficient nonparametric estimation of Toeplitz covariance matrices

Karolina Klockmann¹ Tatyana Krivobokova¹

January 8, 2024

Abstract

A new efficient nonparametric estimator for Toeplitz covariance matrices is proposed. This estimator is based on a data transformation that translates the problem of Toeplitz covariance matrix estimation to the problem of mean estimation in an approximate Gaussian regression. The resulting Toeplitz covariance matrix estimator is positive definite by construction, fully data-driven and computationally very fast. Moreover, this estimator is shown to be minimax optimal under the spectral norm for a large class of Toeplitz matrices. These results are readily extended to estimation of inverses of Toeplitz covariance matrices. Also, an alternative version of the Whittle likelihood for the spectral density based on the discrete cosine transform is proposed. The method is implemented in the R package `vstdct` that accompanies the paper.

Keywords: Discrete cosine transform; Periodogram; Spectral density; Variance-stabilizing transform; Whittle likelihood.

1 Introduction

Estimation of covariance and precision matrices is a fundamental problem in statistical data analysis with countless applications in the natural and social sciences.

¹Department of Statistics and Operations Research, Universität Wien, Oskar-Morgenstern-Platz 1, 1090 Wien, Austria

A special type of covariance matrices that have each descending diagonal constant, known as Toeplitz matrices, arise in the study of stationary stochastic processes. Stationary stochastic processes are an important modeling tool in many applications, such as radar target detection, speech recognition, modeling internet economic activity, electrical brain activity or the motion of crystal structures (Du et al., 2020; Roberts and Ephraim, 2000; Quah, 2000; Franaszczuk et al., 1985; Grenander and Szegö, 1958, p.232).

The data for estimation are given as n independent and identically distributed realizations of a p -dimensional vector having a zero mean and a Toeplitz covariance matrix $\Sigma = (\sigma_{|i-j|})_{i,j=1}^p$. Thereby, p is assumed to grow while n may be equal to 1 or may tend to infinity as well. For $p \rightarrow \infty$ and $p/n \rightarrow c \in (0, \infty]$, the sample (auto-)covariance matrix is known to be an inconsistent estimator of Σ in the spectral norm (see e.g., Wu and Pourahmadi, 2009; Pourahmadi, 2013, chap. 2). Therefore, tapering, banding and thresholding of the sample covariance matrix have been proposed to regularize this estimator (see Wu and Xiao, 2012; Cai et al., 2013). The optimal rate of convergence for Toeplitz covariance matrix estimators was established in Cai et al. (2013), who in particular showed that tapering and banding estimators attain the minimax optimal convergence rate over certain spaces of Toeplitz covariance matrices. Optimality of the thresholded estimator was shown only for the case $n = 1$ (see Wu and Xiao, 2012). However, all of these estimators have several practical drawbacks that affect their performance in small samples. First, additional manipulations with the estimators must be performed to enforce positive definiteness, see e.g., Section 5 in Cai et al. (2013). Second, the data-driven choice of the tapering, banding or thresholding parameter is not trivial in practice. For $n > 1$, Bickel and Levina (2008) proposed a cross-validation criterion that approximates the risk of the estimator. Fang et al. (2016) compared this method with a bootstrap based approximation of the risk in an intensive simulation study and recommended cross-validation over bootstrap. However, for small n a cross-validated tuning parameter turns out to be very variable, while already for moderate n it becomes numerically very demanding. For $n = 1$, to the best of our knowledge, there is no fully data-driven approach for selecting the banding/tapering/thresholding

parameter available. Wu and Pourahmadi (2009) suggested first to split the time series into non-overlapping subseries and then apply the cross-validation criterion of Bickel and Levina (2008). However, it turns out that the appropriate choice of the subseries length is crucial for this approach, but cannot be done data-driven.

In this work, an alternative way to estimate a Toeplitz covariance matrix and its inverse is proposed. Our approach exploits the one-to-one correspondence between Toeplitz covariance matrices and their spectral densities. First, the given data are transformed into approximate Gaussian random variables whose mean equals to the logarithm of the spectral density. Then, the log-spectral density is estimated by a periodic smoothing spline with a data-driven smoothing parameter. Finally, the resulting spectral density estimator is transformed into an estimator for Σ or its inverse. It is shown that this procedure leads to an estimator that is fully data-driven, automatically positive definite and achieves the minimax optimal convergence rate under the spectral norm over a large class of Toeplitz covariance matrices. In particular, this class includes Toeplitz covariance matrices that correspond to long-memory processes with bounded spectral densities. Moreover, the computation is very efficient, does not require iterative or resampling schemes and allows to apply any inference and adaptive estimation procedures developed in the context of nonparametric Gaussian regression.

Estimation of the spectral density from a single stationary time series is a research topic with a long history. Earlier nonparametric methods are based on smoothing the (log-)periodogram, which itself is not a consistent estimator (Bartlett, 1950; Welch, 1967; Thomson, 1982; Wahba, 1980). Another line of nonparametric methods for estimating the spectral density is based on the Whittle likelihood, which is an approximation to the exact likelihood of the time series in the frequency domain. For example, Pawitan and O’Sullivan (1994) estimated the spectral density from a penalized Whittle likelihood, while Kooperberg et al. (1995) used polynomial splines to estimate the log-spectral density function maximizing the Whittle likelihood. Recently, Bayesian methods for spectral density estimation have been proposed (see Choudhuri et al., 2004; Edwards et al., 2019; Maturana-Russel and Meyer, 2021), but these may become very computationally intensive in large samples due to pos-

terior sampling.

The minimax optimal convergence rate for nonparametric estimators of a Hölder continuous spectral density from a single Gaussian stationary time series was obtained by Bentkus (1985) under the L_p norm, $1 \leq p \leq \infty$. Only a few works on spectral density estimation show the optimality of the corresponding estimators. In particular, Kooperberg et al. (1995) and Pawitan and O’Sullivan (1994) derived convergence rates of their estimators for the log-spectral density under the L_2 norm, while neglecting the Whittle likelihood approximation error.

In general, most works on spectral density estimation do not exploit further the close connection to the corresponding Toeplitz covariance matrix estimation. In particular, an upper bound for the L_∞ risk of a spectral density estimator automatically provides an upper bound for the risk of the corresponding Toeplitz covariance matrix estimator under the spectral norm. This fact is used to establish the minimax optimality of our nonparametric estimator for the Toeplitz covariance matrices. The main contribution of this work is to show that our proposed spectral density estimator is not only numerically very efficient, performing excellent in small samples, but also achieves the minimax optimal rate in the L_∞ norm, which in turn ensures the minimax optimality of the corresponding Toeplitz covariance matrix estimator.

The paper is structured as follows. In Section 2, the model is introduced and approximate diagonalization of Toeplitz covariance matrices with the discrete cosine transform is discussed. Moreover, an alternative version of the Whittle’s likelihood is proposed. In Section 3, new estimators for the Toeplitz covariance matrix and the precision matrix are derived, while in Section 4 their theoretical properties are presented. In Section 5, we discuss how the parameters for our estimators are chosen. Section 6 contains simulation results for Gaussian data and in Section 7 the applicability of our method for non-Gaussian data is discussed. Section 8 presents a real data example. The proofs are given in the appendix to the paper. Further simulation studies for non-Gaussian data are attached as supplementary material at the end.

2 Set up and Diagonalization of Toeplitz Matrices

Let $Y_1, \dots, Y_n \stackrel{\text{i.i.d.}}{\sim} \mathcal{N}_p(0_p, \Sigma)$, where Σ is a $p \times p$ positive semi-definite covariance matrix with a Toeplitz structure, that is, $\Sigma = (\sigma_{|i-j|})_{i,j=1}^p \succeq 0$. The sample size n may tend to infinity or be a constant. The case $n = 1$ corresponds to a single observation of a stationary time series and in this case the data are simply denoted by $Y \sim \mathcal{N}_p(0_p, \Sigma)$. The dimension p is assumed to grow. The spectral density function f , corresponding to a Toeplitz covariance matrix Σ with absolute summable sequence of covariances $(\sigma_k)_{k \in \mathbb{Z}}$, is given by

$$f(x) = \sigma_0 + 2 \sum_{k=1}^{\infty} \sigma_k \cos(kx), \quad x \in [-\pi, \pi].$$

The inverse Fourier transform implies

$$\sigma_k = \frac{1}{2\pi} \int_{-\pi}^{\pi} f(x) \cos(kx) dx = \int_0^1 f(\pi x) \cos(k\pi x) dx. \quad (1)$$

If $\sum_{h=-\infty}^{\infty} |\sigma_h| = \infty$, i.e., the corresponding stochastic process is a long-memory process, the spectral density function is directly defined as a 2π -periodic, non-negative function $f : [-\pi, \pi] \rightarrow \mathbb{R}_{\geq 0}$ that satisfies condition (1). Hence, in case f exists, Σ is completely characterized by f . Furthermore, the non-negativity of the spectral density function implies the positive semi-definiteness of the covariance matrix. Moreover, the decay of the covariances σ_k is directly connected to the smoothness of f . Finally, the convergence rate of a Toeplitz covariance estimator and that of the corresponding spectral density estimator are directly related via $\|\Sigma\| \leq \|f\|_{\infty} = \sup_{x \in [-\pi, \pi]} |f(x)|$, where $\|\cdot\|$ denotes the spectral norm (see Grenander and Szegö, 1958, chap. 5.2).

As in Cai et al. (2013), we consider the class of positive semi-definite Toeplitz covariance matrices with Hölder continuous spectral densities. For $\beta = \gamma + \alpha > 0$, where $\gamma \in \mathbb{N} \cup \{0\}$, $0 < \alpha \leq 1$, and $0 < M_0, M_1 < \infty$, let

$$\mathcal{P}_{\beta}(M_0, M_1) = \{f \mid f : [-\pi, \pi] \rightarrow \mathbb{R}_{\geq 0}, \|f\|_{\infty} \leq M_0, \|f^{(\gamma)}(\cdot + h) - f^{(\gamma)}(\cdot)\|_{\infty} \leq M_1 |h|^{\alpha}\}.$$

Furthermore, for $f \in \mathcal{P}_{\beta}(M_0, M_1)$ we denote by $\Sigma(f) \in \mathbb{R}^{p \times p}$ the corresponding

$p \times p$ Toeplitz covariance matrix obtained with the inverse Fourier transform (1) and by $\Sigma^{-1}(f)$ the precision matrix. The optimal convergence rate for estimating Toeplitz covariance matrices $\Sigma(f)$ where $f \in \mathcal{P}_\beta(M_0, M_1)$ depends crucially on β . It is well known that the k th Fourier coefficient of a function whose γ th derivative is Hölder-continuous with exponent $\alpha \in (0, 1]$ decays at least with order $\mathcal{O}(k^{-\beta})$ (see Zygmund, 2002). Hence, β determines the decay rate of the covariances σ_k , which are the Fourier coefficients of the spectral density f , as $k \rightarrow \infty$. For $\beta \in (0, 1/2]$, the class $\mathcal{P}_\beta(M_0, M_1)$ includes bounded spectral densities of certain long-memory processes.

A connection between Toeplitz covariance matrices and their spectral densities is further exploited in the following lemma.

Lemma 1. *Let $\Sigma = \Sigma(f)$ with $f \in \mathcal{P}_\beta(M_0, M_1)$ and $x_j = (j - 1)/(p - 1)$ for $j = 1, \dots, p$. Then*

$$(D^T \Sigma D)_{i,j} = f(\pi x_j) \delta_{i,j} + \frac{1 + (-1)^{|i-j|}}{2} \mathcal{O}(p^{-1} + p^{-\beta} \log p),$$

where $\delta_{i,j}$ is the Kroneker delta, $\mathcal{O}(\cdot)$ terms are uniform over $i, j = 1, \dots, p$ and

$$D = \left(\frac{2}{p-1} \right)^{1/2} \left[\cos \left\{ \pi(i-1) \frac{j-1}{p-1} \right\} \right]_{i,j=1}^p \text{ divided by } 2^{1/2} \text{ when } i \text{ or } j \text{ is } 1 \text{ or } p$$

is the discrete cosine transform I matrix.

The proof can be found in Appendix A.1. This result shows that the discrete cosine transform I matrix approximately diagonalizes Toeplitz covariance matrices and that the diagonalization error depends to some extent on the smoothness of the corresponding spectral density.

In time series analysis the discrete Fourier transform matrix $F = p^{-1/2} \{ \exp(2\pi i j / p) \}_{i,j=1}^p$, where i is the imaginary unit, is typically employed to approximately diagonalize Toeplitz covariance matrices. Using the fact that $(F^T \Sigma F)_{i,i} = f(2\pi i / p) + o(1)$, Whittle (1957) introduced an approximation for the likelihood of a single Gaussian

stationary time series (case $n = 1$), the so-called Whittle likelihood

$$\mathcal{L}(Y|f) \propto \exp \left\{ - \sum_{j=1}^{\lfloor p/2 \rfloor} \log f(2\pi j/p) + \frac{I_j}{f(2\pi j/p)} \right\}. \quad (2)$$

The quantity $I_j = |F_j^T Y|^2$, where F_j denotes the j th column of F , is known as the periodogram at the j th Fourier frequency. Due to periodogram symmetry, only $\lfloor p/2 \rfloor$ data points $I_1, \dots, I_{\lfloor p/2 \rfloor}$ are available for estimating the mean $f(2\pi j/p)$ ($j = 1, \dots, \lfloor p/2 \rfloor$), where $\lfloor x \rfloor$ denotes the largest integer strictly smaller than x . The Whittle likelihood has become a popular tool for parameter estimation of stationary time series, e.g., for nonparametric and parametric spectral density estimation or for estimation of the Hurst exponent, see e.g., Walker (1964); Taqqu and Teverovsky (1997).

Lemma 1 yields the following alternative version of the Whittle likelihood

$$\mathcal{L}(Y|f) \propto \exp \left\{ - \sum_{j=1}^p \log f(\pi x_j) + \frac{W_j}{f(\pi x_j)} \right\}, \quad (3)$$

where $W_j = (D_j^T Y)^2$, with D_j denoting the j th column of D . Note that this likelihood approximation is based on twice as many data points W_j as the standard Whittle likelihood. Thus, it allows for a more efficient use of the data Y to estimate the parameter of interest, such as the spectral density or the Hurst parameter. This is particularly advantageous in small samples.

Equations (2) or (3) invite for the estimation of f by maximizing the (penalized) likelihood over certain linear spaces, e.g., spline spaces, as suggested e.g., in Kooperberg et al. (1995) or Pawitan and O'Sullivan (1994). However, such an approach requires well-designed numerical methods to solve the corresponding optimization problem, since the spectral density in the second term of (2) or (3) is in the denominator, which hinders derivation of a closed-form expression for the estimator and often leads to numerical instabilities. Also, the choice of the smoothing parameter becomes challenging.

Therefore, we suggest an alternative approach that allows the spectral density to

be estimated as a mean in an approximate Gaussian regression. Such estimators have a closed-form expression, do not require an iterative optimization algorithm and a smoothing parameter can be easily obtained with any conventional criterion. First note that if $Y \sim \mathcal{N}_p(0_p, \Sigma)$, with $\Sigma = \Sigma(f)$ and $f \in \mathcal{P}_\beta(M_0, M_1)$, then $D^T Y \sim \mathcal{N}_p(0_p, D^T \Sigma D)$. Hence, for $W_j = (D_j^T Y)^2$ ($j = 1, \dots, p$) it follows with Lemma 1 that

$$W_j \sim \Gamma \left\{ 1/2, 2f(\pi x_j) + \mathcal{O}(p^{-1} + p^{-\beta} \log p) \right\}, \quad (4)$$

where $\Gamma(a, b)$ denotes the gamma distribution with shape parameter a and scale parameter b . The random variables W_1, \dots, W_p are only asymptotically independent. Obviously, $E(W_j) = f(\pi x_j) + o(1)$ for $j = 1, \dots, p$. To estimate f from W_1, \dots, W_p , one could use a generalized nonparametric regression framework with a gamma distributed response, see e.g., the classical monograph by Hastie and Tibshirani (1990). However, this approach requires an iterative procedure for estimation, e.g., a Newton-Raphson algorithm, with a suitable choice for the smoothing parameter at each iteration step. Deriving the L_∞ rate for the resulting estimator is also not a trivial task. Instead, we suggest to employ a variance-stabilizing transform of Cai and Zhou (2010) that converts a gamma regression into an approximate Gaussian regression. In the next section we present the methodology in more detail for a general setting with $n \geq 1$.

3 Methodology

Let $L_\delta = \{f : \inf_x f(x) \geq \delta\}$ for some $\delta > 0$ and set $\mathcal{F}_\beta = \mathcal{P}_\beta(M_0, M_1) \cap L_\delta$. We consider estimation of Σ and $\Omega = \Sigma^{-1}$ from a sample $Y_1, \dots, Y_n \stackrel{\text{i.i.d.}}{\sim} \mathcal{N}_p(0_p, \Sigma)$ where $\Sigma = \Sigma(f)$ with $f \in \mathcal{F}_\beta$. For $Y_i \sim \mathcal{N}_p(0_p, \Sigma)$ ($i = 1, \dots, n$), it was shown in the previous section that with Lemma 1 the data can be transformed into gamma distributed random variables $W_{i,j} = (D_j^T Y_i)^2$ ($i = 1, \dots, n; j = 1, \dots, p$), where for each fixed i the random variable $W_{i,j}$ has the same distribution as W_j given in (4). Now the approach of Cai and Zhou (2010) is adapted to the setting $n \geq 1$.

First, the transformed data points $W_{i,j}$ are binned, that is, fewer new variables

Q_k ($k = 1, \dots, T$), with $T < p$, are built via $Q_k = \sum_{j=(k-1)p/T+1}^{kp/T} \sum_{i=1}^n W_{i,j}$ for $k = 1, \dots, T$. Note that the number of observations in a bin is $m = np/T$. In Theorem 1 in Section 4, we show that setting $T = \lfloor p^\nu \rfloor$ for any $\nu \in (1 - \min\{1, \beta\}/3, 1)$ leads to the minimax optimal rate for the spectral density estimator. To simplify the notation, m is handled as an integer (otherwise, one can discard several observations in the last bin). Next, applying the variance-stabilizing transform $G(x) = 2^{-1/2} \log(x/m)$ to each Q_k yields new random variables $Y_k^* = 2^{-1/2} \log(Q_k/m)$ that are approximately Gaussian, as shown in Cai and Zhou (2010). Since the spectral density is a function that is symmetric around zero and periodic on $[-\pi, \pi]$, one can mirror the resulting observations to use $Y_T^*, \dots, Y_2^*, Y_1^*, \dots, Y_{T-1}^*$ for estimation. Renumerating the observations Y_k^* and scaling the design points into the interval $[0, 1)$ for convenience leads to an approximate Gaussian regression problem

$$Y_k^* \stackrel{\text{approx.}}{\sim} \mathcal{N} [H \{f(x_k)\}, m^{-1}], \quad x_k = \frac{k-1}{2T-2} \quad (k = 1, \dots, 2T-2),$$

where $H(y) = 2^{-1/2} \{\phi(m/2) + \log(2y/m)\}$ and ϕ is the digamma function, see Cai and Zhou (2010). Now, the scaled and shifted log-spectral density $H(f)$ can be estimated with a periodic smoothing spline

$$\widehat{H(f)}(x) = \arg \min_{s \in S_{\text{per}}(2q-1)} \left[\frac{1}{2T-2} \sum_{k=1}^{2T-2} \{Y_k^* - s(x_k)\}^2 + h^{2q} \int_0^1 \{s^{(q)}(x)\}^2 dx \right], \quad (5)$$

where $h > 0$ denotes a smoothing parameter, $q \in \mathbb{N}$ is the penalty order and $S_{\text{per}}(2q-1)$ is a space of periodic splines of degree $2q-1$. More details on periodic smoothing splines can be found in Appendix A.2.

Once an estimator $\widehat{H(f)}$ is obtained, application of the inverse transform function $H^{-1}(y) = m \exp\{2^{1/2}y - \phi(m/2)\}/2$ yields the spectral density estimator $\hat{f} = H^{-1}\{\widehat{H(f)}\}$. Finally, the inverse Fourier transform leads to the following covariance matrix estimator

$$\widehat{\Sigma} = (\hat{\sigma}_{|i-j|})_{i,j=1}^p, \quad \text{with } \hat{\sigma}_k = \int_0^1 \hat{f}(x) \cos(k\pi x) dx \text{ for } k = 0, \dots, p-1. \quad (6)$$

The precision matrix Ω is estimated by the inverse Fourier transform of the reciprocal

of the spectral density estimator, i.e.,

$$\widehat{\Omega} = (\widehat{\omega}_{|i-j|})_{i,j=1}^p, \text{ with } \widehat{\omega}_k = \int_0^1 \widehat{f}(x)^{-1} \cos(k\pi x) dx \text{ for } k = 0, \dots, p-1. \quad (7)$$

The estimation procedure for $\widehat{\Sigma}$ and $\widehat{\Omega}$ can be summarized as follows.

1. **Data transformation:** Define $W_{i,j} = (D_j^T Y_i)^2$ ($i = 1, \dots, n; j = 1, \dots, p$), where D is the $p \times p$ discrete cosine transform I matrix as given in Lemma 1 and D_j is its j th column.

2. **Binning:** Set $T = \lfloor p^v \rfloor$ for any $v \in (1 - \min\{1, \beta\}/3, 1)$ and calculate

$$Q_k = \sum_{j=(k-1)p/T+1}^{kp/T} \sum_{i=1}^n W_{i,j}, \quad (k = 1, \dots, T).$$

3. **Variance-stabilizing transform:** Set $Y_k^* = 2^{-1/2} \log(Q_k/m)$ for $k = 1, \dots, T$ and $m = np/T$. Mirror the data to get $2T-2$ approximately Gaussian random variables $Y_T^*, \dots, Y_2^*, Y_1^*, \dots, Y_{T-1}^*$.

4. **Gaussian regression:** Renumerate observations Y_k^* , scale the design points to $[0, 1)$, and estimate $H(f)$ with a periodic smoothing spline of degree $2q-1$ in an approximate Gaussian regression model

$$Y_k^* = H\{f(x_k)\} + \epsilon_k, \quad x_k = \frac{k-1}{2T-2} \quad (k = 1, \dots, 2T-2),$$

where ϵ_k are asymptotically i.i.d. Gaussian variables.

5. **Inverse transform:** Estimate the spectral density f with $\widehat{f} = H^{-1}\{\widehat{H}(f)\}$, where

$$H^{-1}(y) = m \exp\{2^{1/2}y - \phi(m/2)\} / 2, \text{ for a digamma function } \phi.$$

6. **Estimators:** Set $\widehat{\Sigma} = (\widehat{\sigma}_{|i-j|})_{i,j=1}^p$ with $\widehat{\sigma}_k = \int_0^1 \widehat{f}(x) \cos(k\pi x) dx$ and $\widehat{\Omega} = (\widehat{\omega}_{|i-j|})_{i,j=1}^p$ with $\widehat{\omega}_k = \int_0^1 \widehat{f}(x)^{-1} \cos(k\pi x) dx$ ($k = 0, \dots, p-1$).

The estimators $\widehat{\Sigma}$ and $\widehat{\Omega}$ are positive definite matrices by construction, since the spectral density estimator \widehat{f} is non-negative by definition. For a detailed discussion on the choice of all parameters needed to obtain our estimators see Section 5.

4 Theoretical Properties

In this section, we study the asymptotic properties of the estimators \hat{f} , $\hat{\Sigma}$ and $\hat{\Omega}$. Let $\hat{f} = m \exp\{2^{1/2}\widehat{H}(f) - \phi(m/2)\}/2$ be the spectral density estimator defined in Section 3, where $\widehat{H}(f)$ is given in (5), $m = np/T$ and ϕ is the digamma function. Furthermore, let $\hat{\Sigma}$ be the Toeplitz covariance matrix estimator and $\hat{\Omega}$ the corresponding precision matrix defined in equations (6) and (7), respectively. The following theorem shows that both $\hat{\Sigma}$ and $\hat{\Omega}$ attain the minimax optimal rate of convergence over the class of Toeplitz matrices $\Sigma(f)$ such that $f \in \mathcal{F}_\beta$, $\beta > 0$.

Theorem 1. *Let $Y_1, \dots, Y_n \stackrel{i.i.d.}{\sim} \mathcal{N}_p(0_p, \Sigma)$, $n \geq 1$, with $\Sigma = \Sigma(f)$ such that $f \in \mathcal{F}_\beta$ and $\beta = \gamma + \alpha > 0$. If $h > 0$ such that $h \rightarrow 0$ and $hT \rightarrow \infty$, then with $T = \lfloor p^v \rfloor$ for any $v \in (1 - \min\{1, \beta\}/3, 1)$ and $q = \max\{1, \gamma\}$, the spectral density estimator \hat{f} , the corresponding covariance matrix estimator $\hat{\Sigma}$ and the precision matrix estimator $\hat{\Omega}$ satisfy for $p \rightarrow \infty$ and n such that $p^{\min\{1, \beta\}}/n \rightarrow c \in (0, \infty]$*

$$\begin{aligned} \sup_{f \in \mathcal{F}_\beta} E_f \|\hat{\Sigma} - \Sigma(f)\|^2 &\leq \sup_{f \in \mathcal{F}_\beta} E_f \|\hat{f} - f\|_\infty^2 = \mathcal{O} \left\{ \frac{\log(np)}{nph} \right\} + \mathcal{O}(h^{2\beta}) \\ \sup_{f \in \mathcal{F}_\beta} E_f \|\hat{\Omega} - \Sigma^{-1}(f)\|^2 &= \mathcal{O} \left\{ \frac{\log(np)}{nph} \right\} + \mathcal{O}(h^{2\beta}). \end{aligned}$$

For $h \asymp \{\log(np)/(np)\}^{\frac{1}{2\beta+1}}$ it follows that

$$\begin{aligned} \sup_{f \in \mathcal{F}_\beta} E_f \|\hat{\Sigma} - \Sigma(f)\|^2 &\leq \sup_{f \in \mathcal{F}_\beta} E_f \|\hat{f} - f\|_\infty^2 = \mathcal{O} \left[\left\{ \frac{\log(np)}{np} \right\}^{\frac{2\beta}{2\beta+1}} \right] \\ \sup_{f \in \mathcal{F}_\beta} E_f \|\hat{\Omega} - \Sigma^{-1}(f)\|^2 &= \mathcal{O} \left[\left\{ \frac{\log(np)}{np} \right\}^{\frac{2\beta}{2\beta+1}} \right]. \end{aligned}$$

Theorem 1 is established under the asymptotic scenario with $p \rightarrow \infty$ and n such that $p^{\min\{1, \beta\}}/n \rightarrow c \in (0, \infty]$, i.e., the dimension p grows, while the sample size n either remains fixed or also grows but not faster than $p^{\min\{1, \beta\}}$. Note that this asymptotic scenario covers the setting when the sample covariance matrix is inconsistent. In particular, for $\beta \geq 1$ the sample size n does not grow faster than p and adding more samples improves the convergence rate. If $\beta \in (0, 1)$, then increasing n with the rate faster than p^β will not lead to a faster convergence rate, due to the diagonalization

error from Lemma 1, which can be improved only by making additional assumptions on the spectral density.

The minimax optimal convergence rates for estimating Σ and Σ^{-1} from n i.i.d. Gaussian vectors Y_1, \dots, Y_n with zero mean and a Toeplitz covariance matrix $\Sigma(f)$ with $f \in \mathcal{F}_\beta$ have been established by (Cai et al., 2013). Since the lower bound rates given in Theorems 5 and 7 in (Cai et al., 2013) match the upper bound rates obtained in our Theorem 1, we conclude that our estimator is minimax optimal. For non-Gaussian data the minimax optimal convergence rates for Σ and Σ^{-1} are not known. Note that \mathcal{F}_β with $\beta > 0$ includes bounded spectral densities of long-memory processes.

The proof of Theorem 1 can be found in Appendix A.3 and is the main result of our work. The most important part of this proof is the derivation of the convergence rate for the spectral density estimator \hat{f} under the L_∞ norm. In the original work, Cai and Zhou (2010) established an L_2 rate for a wavelet nonparametric mean estimator in a gamma regression where the data are assumed to be independent. In our work, the spectral density estimator \hat{f} is based on the gamma distributed data $W_{i,1}, \dots, W_{i,p}$, which are only asymptotically independent. Moreover, the mean of these data is not exactly $f(\pi x_1), \dots, f(\pi x_p)$, but is corrupted by the diagonalization error given in Lemma 1. This error adds to the error that arises via binning and VST and that describes the deviation from a Gaussian distribution, as derived in Cai and Zhou (2010). Finally, we need to obtain an L_∞ rather than an L_2 rate for our spectral density estimator. Overall, the proof requires different and partly novel tools than those used in Cai and Zhou (2010). A particular challenge is the treatment of the dependence of $W_{i,1}, \dots, W_{i,p}$.

To get the L_∞ rate for \hat{f} , we first derive that for the periodic smoothing spline estimator $\widehat{H}(f)$ of the log-spectral density. To do so, we use a closed-form expression of its effective kernel obtained in Schwarz and Krivobokova (2016), thereby carefully treating various (dependent) errors that describe deviations from a Gaussian nonparametric regression with independent errors and mean $f(\pi x_i)$. Note also that although the periodic smoothing spline estimator is obtained on T binned points, the

rate is given in terms of the vector dimension p and the sample size n . Next, using the Cauchy-Schwarz inequality and a mean value argument, this rate is translated into the L_∞ rate for the spectral density estimator \hat{f} . To obtain the rate for the Toeplitz covariance matrix estimator is enough to note that $E\|\widehat{\Sigma}-\Sigma\|^2 \leq E\|\hat{f}-f\|_\infty^2$.

5 Practical Issues

Several choices must be made in practice to obtain our estimator. First, the data Y_i ($i = 1, \dots, n$) are transformed into $W_{i,j} = (D_j^T Y_i)^2$ ($j = 1, \dots, p$) and are subsequently binned. According to Theorem 1, the number of bins $T = \lfloor p^v \rfloor$ with any $v \in (1 - \min\{\beta, 1\}/3, 1)$ leads to a minimax optimal estimator. That is, for $\beta \geq 1$ one can take any $v \in (2/3, 1)$, while for $\beta < 1$ the interval depends on β , for example, for $\beta = 1/2$ the interval is $v \in (5/6, 1)$. In our simulation studies we observed that the results are quite robust for various values for v . If no knowledge about β is available, one can proceed as follows. Any standard test for long-range dependence can be performed and if the null hypothesis of long-range dependence is rejected, i.e., $\beta > 1/2$, then any $v \in (5/6, 1)$ can be taken. Otherwise, a smaller interval for v should be considered. Additionally, one can always verify whether the chosen value of T is appropriate by generating QQ-plots of Y_k^* , which ideally should show little departure from the normality. Several figures in the Supplementary Material show how the QQ-plots change for Gaussian data depending on T .

Once the data are transformed, the mean of Y_k^* ($k = 1, \dots, T$), i.e., the log-spectral density, is estimated with a periodic smoothing spline. For this, one needs to choose basis functions of the periodic spline space, the penalty order $q \in \mathbb{N}$ and the smoothing parameter $h > 0$.

The basis of a periodic spline space with knots put at the observations is a Fourier basis $\{2^{1/2} \cos(2\pi x), 2^{1/2} \sin(2\pi x)\}$, evaluated at $x_k = (k - 1)/(2T - 2)$ for $k = 1, \dots, 2T - 2$.

The smoothing parameter h can be chosen using any data-driven approach, such as (generalized) cross-validation or an empirical Bayes approach, see Wahba (1985).

According to Theorem 1, the choice of q should be related to the true smoothness β of the spectral density in order to obtain the minimax optimal estimator. Assume that q taken for estimation is larger than the true smoothness β . Then, the rate of convergence is determined by the true β and is minimax, independent on how large q is. In particular, if $\gamma = 0$, then $\beta = \alpha \in (0, 1)$ and taking $q = \max\{1, \gamma\} = 1$ would lead to a minimax optimal estimator. If q taken for the estimation is less than β , then the rate will depend on q and on the choice of the smoothing parameter h . Assume that $\beta > q$ and the smoothing parameter h is estimated with (generalized) cross-validation. Then, it has been shown in (Wahba, 1985) that a periodic spline estimator adapts to the unknown smoothness up to $2q$. That is, if $\beta < 2q$, then the rate will be minimax optimal, while for $\beta \geq 2q$ the rate will be determined by q . If $\beta > q$ and the smoothing parameter h is estimated by the empirical Bayesian approach, then (Wahba, 1985) has shown that the resulting estimator does not adapt to the extra smoothness. However, in small samples the empirical Bayes smoothing spline can perform similar or even better than the cross-validated smoothing spline due to smaller constants in the risk, see (Krivobokova, 2013).

Since in practice β is not known exactly, it is also not known which rate the estimator will have with a chosen q . However, looking at the decay of the sample covariance functions one can get an idea whether β is rather small, in case of a very slow decay, or rather large, in case of a very fast decay, and decide on the choice of q . A more attractive approach is to resort to adaptive estimation methods, that lead to the best possible estimators without prior knowledge on β . For example, the empirical Bayesian framework allows to estimate the unknown γ under certain assumptions on the function space (Serra et al., 2017). Other approaches for adaptive non-parametric estimation are aggregation and Lepski's method, see e.g., (Chagny, 2016) for an overview and references. A detailed study of adaptive spectral density estimators is out of scope of our work.

In our simulation study and the real data example, presented in the next two sections, we discuss the parameter choices explicitly.

6 Simulation Study

In this section, we compare the performance of our proposed Toeplitz covariance estimator with the tapering estimator of Cai et al. (2013) and with the sample covariance matrix. A Monte Carlo simulation with 100 samples is performed using R (version 4.1.2, seed 42). We consider Gaussian vectors $Y_1, \dots, Y_n \stackrel{\text{i.i.d.}}{\sim} \mathcal{N}_p(0_p, \Sigma)$ with (A) $p = 5000, n = 1$, (B) $p = 1000, n = 50$ and (C) $p = 5000, n = 10$, and with the covariance functions $\sigma : \mathbb{Z} \rightarrow \mathbb{R}, k \mapsto \sigma_k$

- (1) of a polynomial decay, i.e., $\sigma_k = 1.44(1 + |k|)^{-5.1}$,
- (2) of an autoregressive process $y_t = \epsilon_t + 0.1y_{t-1} - 0.1y_{t-2}$ where ϵ_t is i.i.d. Gaussian noise and $\text{var}(\epsilon_t) = 1.44$,
- (3) such that the corresponding spectral density is Lipschitz continuous but not differentiable: $f(x) = 1.44\{|\sin(x + 0.5\pi)|^{1.7} + 0.45\}$.

In particular, $\sigma_0 = 1.44$ in all three examples. Figure 1 shows the spectral densities and the corresponding covariance functions for the three examples. To set the parameters note that the spectral density of the process (1) belongs to \mathcal{F}_4 , the spectral density of the process (2) is an analytic function and the spectral density of the process (3) is from \mathcal{F}_1 .

Since for all three processes $\beta \geq 1$, according to Theorem 1, any value of $v \in (2/3, 1)$ should lead to optimal estimation. We set the number of bins to $T = 500$ bins in all scenarios, which corresponds to $v \approx 0.73$ for scenario (A) and (C) and $v \approx 0.90$ for scenario (B).

Setting $q = 2$ would lead to the minimax optimal rates for processes (1) and (3), if the smoothing parameter is chosen by (generalized) cross-validation, see discussion in Section 5. According to arguments from the previous section, the convergence rate for the process (2) is the same as that for the process (1), while process (3) has a slower convergence rate. Hence, for a given scenario, we should observe similar magnitude of the average norms for processes (1) and (2), while somewhat larger

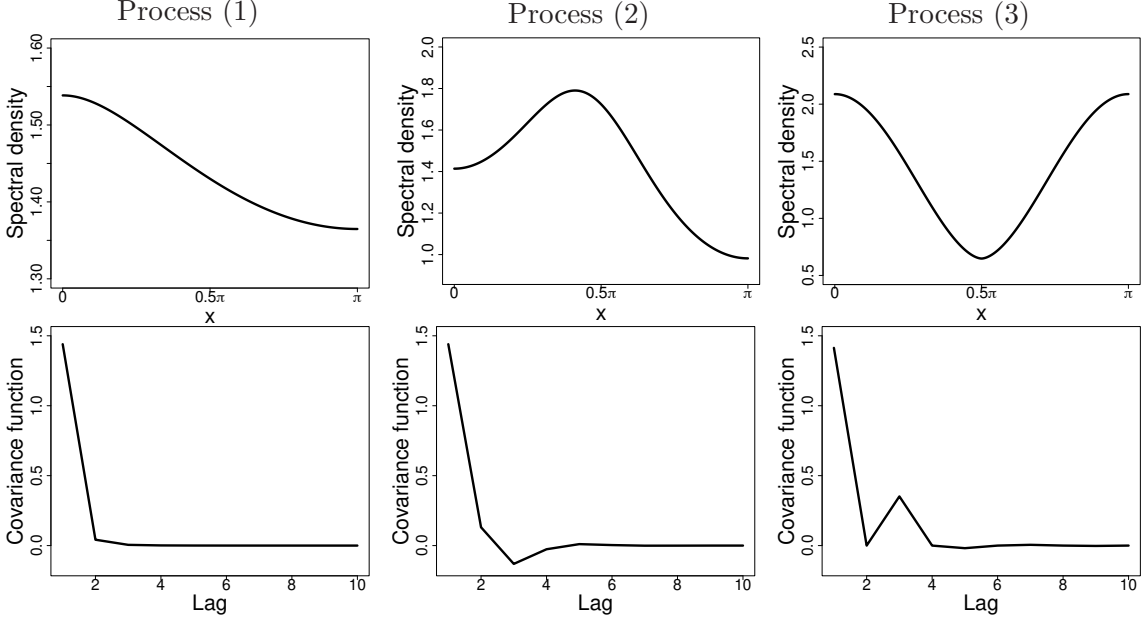


Figure 1: Spectral density functions (first row) and covariance functions (second row) for examples (1)–(3).

values for process (3). Across scenarios, we expect scenario (A) to have larger values of the average norms, as only $p = 5\,000$ observations are used, compared to $np = 50\,000$ data points in scenarios (B) and (C).

To select the regularization parameter for our estimator, we implemented the restricted maximum likelihood method, generalized cross-validation and the corresponding oracle versions, i.e., as if Σ were known.

The sample covariance matrix $\tilde{\Sigma} = (\tilde{\sigma}_{|i-j|})_{i,j=1}^p$ is defined as $n^{-1} \sum_{i=1}^n Y_i Y_i^T$ with averaged diagonals to obtain Toeplitz structure. The tapering estimator with tapering parameter $k \leq p/2$ is defined as $\text{Tap}_k(\tilde{\Sigma}) = (\tilde{\sigma}_{|i-j|} w_{|i-j|})_{i,j=1}^p$, where $w_m = 1$ when $m = 0, \dots, k/2$, $w_m = 2 - 2m/k$ when $k/2 < m \leq k$ and otherwise $w_m = 0$, see Cai et al. (2013). The parameter k can be selected using cross-validation (see Bickel and Levina, 2008) only if $n > 1$, that is, under scenarios (B) and (C). For this, the n observations are divided by 30 random splits into a training set of size $n_1 = 2n/3$ and a test set of size $n_2 = n/3$. Let Σ_1^y and Σ_2^y be the sample covariance

matrices from the ν th split. The tapering parameter k is then estimated as

$$\hat{k}_{\text{cv}} = \arg \min_{k=2,3,\dots,p/2} \frac{1}{30} \sum_{\nu=1}^{30} \|\text{Tap}_k(\Sigma_1^\nu) - \Sigma_2^\nu\|,$$

where $\text{Tap}_k(\Sigma_2^\nu)$ is the tapering estimator with parameter k . If $n = 1$, that is, under scenario (A), Wu and Pourahmadi (2009) suggest to split the time series Y into l non-overlapping subseries of length p/l and then proceed as before to select the tuning parameter k . To the best of our knowledge, there is no data-driven method for the selection of l . Using the true covariance matrix Σ , we preselected oracle values $l = 30$ subseries for the example (1) and $l = 15$ subseries for the examples (2) and (3). The parameter k can then be chosen with cross-validation as above. We employ this approach under scenario (A) instead of an unavailable fully data-driven criterion and name it semi-oracle. Finally, for all three scenarios (A), (B) and (C), the oracle tapering parameter is computed using grid search for each Monte Carlo sample as $\hat{k}_{\text{or}} = \arg \min_{k=2,3,\dots,p/2} \|\text{Tap}_k(\tilde{\Sigma}) - \Sigma\|$, where $\tilde{\Sigma}$ is the sample covariance matrix. To speed up the computation, one can replace the spectral norm by the ℓ_1 norm, as suggested by Bickel and Levina (2008).

Table 1: (A) $p = 5000$, $n = 1$: Errors of the Toeplitz covariance matrix and the spectral density estimators with respect to the spectral and the L_2 norm; average computation time of the covariance estimators in seconds for one Monte Carlo sample is in the last column; all numbers multiplied with 100 except the last column

	Process (1)		Process (2)		Process (3)		time in sec
	$\ \hat{\Sigma} - \Sigma\ ^2$	$\ \hat{f} - f\ _2^2$	$\ \hat{\Sigma} - \Sigma\ ^2$	$\ \hat{f} - f\ _2^2$	$\ \hat{\Sigma} - \Sigma\ ^2$	$\ \hat{f} - f\ _2^2$	
our method (GCV)	0.688	0.255	1.591	0.439	3.401	0.606	4.235
our method (ML)	0.591	0.224	1.559	0.417	3.747	0.628	4.224
tapering (semi-oracle)	0.558	0.216	2.325	0.674	3.551	0.979	4.617
sample covariance	16240.895	3810.680	20291.809	3694.392	24438.036	3809.486	0.342
our method (GCV-oracle)	0.421	0.175	1.373	0.378	3.321	0.575	
our method (ML-oracle)	0.464	0.186	1.487	0.391	3.781	0.624	
tapering (oracle)	0.418	0.171	1.045	0.288	1.547	0.371	

In Tables 1, 2 and 3, the errors of the Toeplitz covariance estimators with respect to the spectral norm and the average computation time for one Monte Carlo sample for all three processes are reported for scenarios (A), (B) and (C), respectively. To illustrate the goodness-of-fit of the spectral density, the L_2 norm $\|\hat{f} - f\|_2$ is also computed.

Table 2: (B) $p = 1000, n = 50$: Errors of the Toeplitz covariance matrix and the spectral density estimators with respect to the spectral and the L_2 norm; average computation time of the covariance estimators in seconds for one Monte Carlo sample is in the last column; all numbers multiplied with 100 except the last column

	Process (1)		Process (2)		Process (3)		time in sec
	$\ \widehat{\Sigma} - \Sigma\ ^2$	$\ \widehat{f} - f\ _2^2$	$\ \widehat{\Sigma} - \Sigma\ ^2$	$\ \widehat{f} - f\ _2^2$	$\ \widehat{\Sigma} - \Sigma\ ^2$	$\ \widehat{f} - f\ _2^2$	
our method (GCV)	0.100	0.028	0.205	0.050	0.531	0.082	27.194
our method (ML)	0.076	0.024	0.230	0.051	0.611	0.089	27.098
tapering (CV)	0.110	0.031	0.218	0.055	0.348	0.073	23.908
sample covariance	79.603	56.262	95.090	61.000	127.528	61.001	0.141
our method (GCV-oracle)	0.062	0.020	0.163	0.043	0.462	0.074	
our method (ML-oracle)	0.067	0.021	0.221	0.050	0.603	0.088	
tapering (oracle)	0.057	0.020	0.133	0.037	0.265	0.055	

Table 3: (C) $p = 5000, n = 10$: Errors of the Toeplitz covariance matrix and the spectral density estimators with respect to the spectral and the L_2 norm; average computation time of the covariance estimators in seconds for one Monte Carlo sample is in the last column; all numbers multiplied with 100 except the last column

	Process (1)		Process (2)		Process (3)		time in sec
	$\ \widehat{\Sigma} - \Sigma\ ^2$	$\ \widehat{f} - f\ _2^2$	$\ \widehat{\Sigma} - \Sigma\ ^2$	$\ \widehat{f} - f\ _2^2$	$\ \widehat{\Sigma} - \Sigma\ ^2$	$\ \widehat{f} - f\ _2^2$	
our method (GCV)	0.088	0.026	0.217	0.050	0.593	0.079	4.260
our method (ML)	0.078	0.023	0.231	0.050	0.677	0.086	4.251
tapering (CV)	0.143	0.034	0.217	0.051	0.422	0.070	635.345
sample covariance	673.122	370.946	792.714	360.687	1014071.587	375.728	1.189
our method (GCV-oracle)	0.062	0.020	0.172	0.043	0.500	0.071	
our method (ML-oracle)	0.069	0.021	0.224	0.048	0.663	0.085	
tapering (oracle)	0.055	0.018	0.147	0.039	0.257	0.051	

The overall behavior of our estimator is exactly as expected. Moreover, the tapering and our estimator perform similar in terms of the spectral norm risk. This is not surprising as both estimators are proved to be rate-optimal. The oracle estimators show similar behavior, but are slightly less variable compared to the data-driven estimators. Clearly, both the tapering and our estimators are superior to the inconsistent sample covariance matrix. In terms of computational time, both methods are similarly fast for scenarios (A) and (B). For scenario (C), the tapering method is much slower due to the multiple high-dimensional matrix multiplications in the cross-validation method. It is anticipated that for larger p the tapering estimator is much more computationally intensive compared to our method.

7 Application to Non-Gaussian Data

While we consider the rigorous theoretical study of our estimator for non-Gaussian data to be out of scope of this work, we would like to discuss in this section the application of our method to non-Gaussian data in practice.

To apply our method, one needs to ensure that the transformed data Y_k^* are approximately Gaussian with mean $H\{f(x_k)\}$. Our estimator will be minimax optimal if the deviation from Gaussianity of Y_k^* is sufficiently small. In general, one needs to ensure that

- (i) the mean of $(D_j^T Y_i)^2$ is the spectral density up to a negligible error $f(\pi x_j)\{1 + o(1)\}$,
- (ii) the central limit theorem is applicable to Q_k after appropriate centering and scaling,
- (iii) the log-transform is variance-stabilizing for $(D_j^T Y_i)^2$.

The first point is always satisfied, as long as both moments of $D_j^T Y_i$ exist. Indeed, suppose that Y_i has a Toeplitz covariance matrix Σ and the marginal distribution is non-Gaussian with mean zero. Then, $E\{(D_j^T Y_i)^2\} = (D^T \Sigma D)_{jj} = f(\pi x_j)\{1 + o(1)\}$. The last two points can be checked explicitly, if the distribution of Y_i is known. For example, for gamma distributed data the second point is clearly satisfied and the third point is proved in the Supplementary Material.

Of course, in practice the distribution of Y_i is rarely known. Since our method relies on the asymptotic normality of Y_k^* , one can simply check whether the data deviate from normality strongly. Note that application of normality tests for Y_k^* might be misleading in small samples, since Y_k^* are only asymptotically Gaussian, even when Y_i are Gaussian. Therefore, we suggest to generate a QQ-plot of Y_k^* . If this QQ-plot shows little deviations from Gaussianity, then our method can safely be applied in practice. If deviations from normality are substantial, this might indicate that the log-transform of the data is not suitable. To find an appropriate variance-stabilizing

transformation, one can employ a Box-Cox transform. Note that to estimate the Box-Cox transformation parameter, one must take into account correlation of the binned data, e.g., by using the method of (Guerrero, 1993) developed for time series.

In the Supplementary Material we provide a small simulation study, as well as several QQ-plots of Y_k^* , where the distribution of $\Sigma^{-1/2}Y_i$ was taken to be gamma and uniform. It can be observed that in all examples the QQ-plots show little departure from the Gaussian distribution and all simulation results look very similar independent on the distribution of Y_i .

8 Application to Protein Dynamics

We revisit the data analysis of protein dynamics performed in Krivobokova et al. (2012) and Singer et al. (2016). We consider data generated by the molecular dynamics simulations for the yeast aquaporin, the gated water channel of the yeast *Pichi pastoris*. Molecular dynamics simulations are an established tool for studying biological systems at the atomic level on timescales of nano- to microseconds. The data are given as Euclidean coordinates of all 783 atoms of the aquaporin observed in a 100 nanosecond time frame, split into 20 000 equidistant observations. Additionally, the diameter of the channel y_t at time t is given, measured by the distance between two centers of mass of certain residues of the protein. The aim of the analysis is to identify the collective motions of the atoms responsible for the channel opening. In order to model the response variable y_t , which is a distance, based on the motions of the protein atoms, we chose to represent the protein structure by distances between atoms and certain fixed base points instead of Euclidean coordinates. That is, we calculated

$$X_t = \{d(A_{t,1}, B_1), \dots, d(A_{t,783}, B_1), d(A_{t,1}, B_2), \dots, d(A_{t,783}, B_y)\} \in \mathbb{R}^{4 \cdot 783},$$

where $A_{t,i} \in \mathbb{R}^3$, $i = 1, \dots, 783$ denotes the i th atom of the protein at time t , $B_j \in \mathbb{R}^3$ ($j = 1, \dots, 4$), is the j th base point and $d(\cdot, \cdot)$ is the Euclidean distance. Figure 2 shows the diameter y_t and the distance between the first atom and the first center of mass.

It can be concluded that a linear model $Y = Xb + \epsilon$ holds, where $Y = (y_1, \dots, y_{20000})^T$,

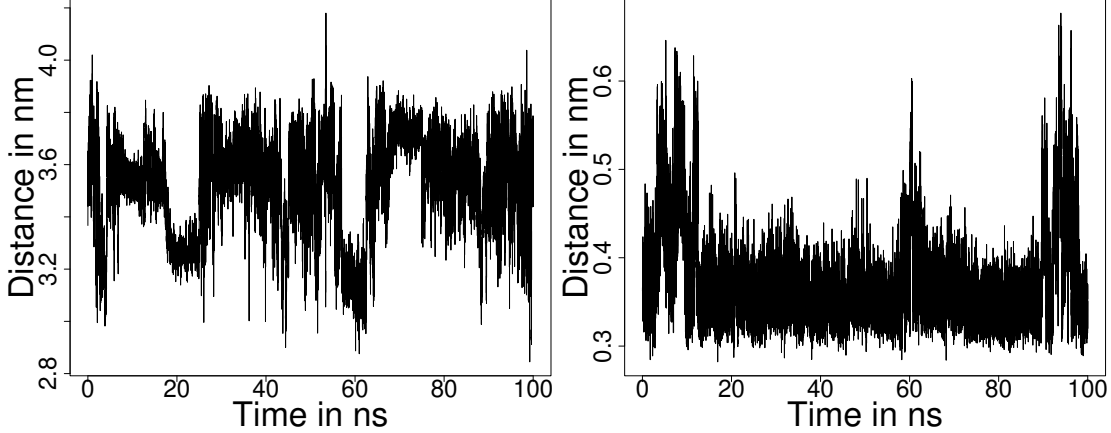


Figure 2: Distance between the first atom and the first center of mass of aquaporin (left) and the opening diameter y_t over time t (right).

$X = (X_1^T, \dots, X_{20000}^T)^T$, $b \in \mathbb{R}^{4783}$, $\epsilon \in \mathbb{R}^{20000}$. This linear model has two specific features which are intrinsic to the problem: first, the observations are not independent over time and second, X_t is high-dimensional at each t and only few columns of X are relevant for Y . Krivobokova et al. (2012) have shown that the partial least squares (PLS) algorithm performs exceptionally well on this type of data, leading to a small-dimensional and robust representation of proteins, which is able to identify the atomic dynamics relevant for Y . Singer et al. (2016) studied the convergence rates of the PLS algorithm for dependent observations and showed that decorrelating the data before running the PLS algorithm improves its performance. Since Y is a linear combination of columns of X , it can be assumed that Y and all columns of X have the same correlation structure. Hence, it is sufficient to estimate $\Sigma = \text{cov}(Y)$ to decorrelate the data for the PLS algorithm, i.e., $\Sigma^{-1/2}Y = \Sigma^{-1/2}Xb + \Sigma^{-1/2}\epsilon$ results in a standard linear regression with independent errors.

Our goal now is to estimate Σ and compare the performance of the PLS algorithm on original and decorrelated data. For this purpose, we divided the data set into a training and a test set, each with $p = 10\,000$ observations. First, we tested whether the data are stationary. The augmented Dickey-Fuller test confirmed stationarity for Y with a p -value < 0.01 . The Hurst exponent of Y is 0.85, indicating moderate long-range dependence supported by a rather slow decay of the sample covariances,

see the grey line in the left plot of Fig. 3. Therefore, we set $q = 1$ for our estimator to match the low smoothness of the corresponding spectral density. Application of the R package `forecast`, that implements the approach of Guerrero (1993) to estimate the Box-Cox transform parameter, confirms that the log-transform is appropriate for these data. The bin number is set to $T = 2500$, i.e., $v \approx 0.85$. The smoothing parameter of the log-spectral density is selected with generalized cross-validation. The black line in the left plot of Fig. 3 confirms that the covariance matrix estimated with our method almost completely decorrelates the channel diameter Y on the training data set. Next, we estimated the regression coefficients b with the usual partial least squares algorithm, ignoring the dependence in the data. Finally, we estimated b with the partial least squares algorithm that takes into account dependence using our covariance estimator $\hat{\Sigma}$. Based on these regression coefficient estimators, the prediction on the test set was calculated. The plot on the right side of Fig. 2 shows the Pearson correlation between the true channel diameter on the test set and the prediction on the same test set based on raw (in grey) and decorrelated data (in black). Obviously, the performance of the partial least squares algorithm on the decorrelated data is significantly better for smaller numbers of components. In particular, with just one component, the correlation between the true opening diameter on the test set and its prediction that takes into account the dependence in the data is already 0.45, while it is close to zero for the partial least squares method that ignores the dependence in the data. Krivobokova et al. (2012) showed that the estimator of b based on one PLS component is exactly the ensemble-weighted maximally correlated mode, which is defined as the collective mode of atoms that has the highest probability to achieve a specific alteration of the response Y . Therefore, an accurate estimator of this quantity is crucial for the interpretation of the results and can only be achieved if the dependence in the data is taken into account.

Estimating Σ with a tapered covariance estimator has two practical problems. First, since we only have a single realization of a time series Y , i.e., $n = 1$, there is no data-driven method for selecting the tapering parameter. Second, the tapering estimator turned out to be not positive definite for the data at hand. To solve the second problem, we truncated the corresponding spectral density estimator \hat{f}_{tap} to a small posi-

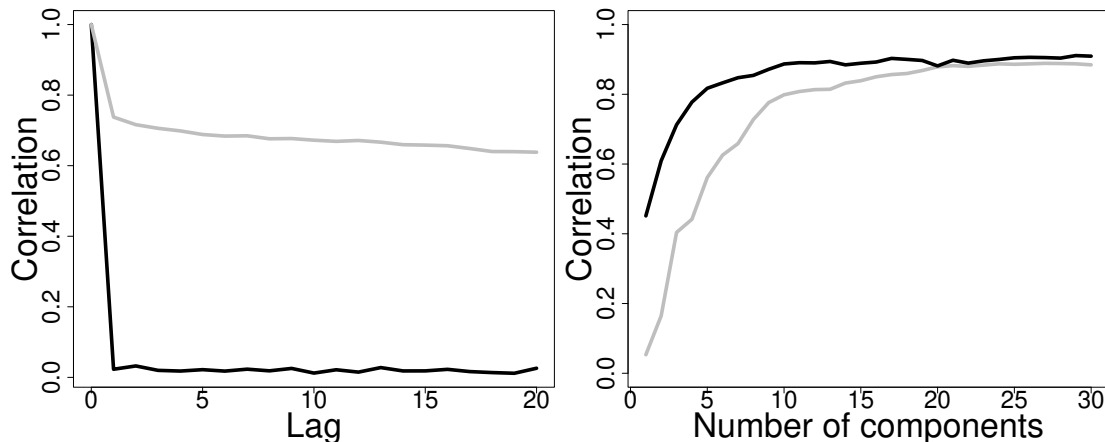


Figure 3: On the left, the correlation function of Y (grey) and of $\hat{\Sigma}^{-1/2}Y$ (black), where $\hat{\Sigma}$ is estimated with our method; On the right, correlation between the true values on the test data set and prediction based on partial least squares (grey) and corrected partial least squares (black).

tive value, i.e., $\hat{f}_{\text{tap}}^+ = \max\{\hat{f}_{\text{tap}}, 1/\log p\}$ (see Cai et al., 2013; McMurry and Politis, 2010). To select the tapering parameter with cross-validation, we experimented with different subseries lengths and found that the tapering estimator is very sensitive to this choice. For example, estimating the tapered covariance matrix based on subseries of length 8/15/30 yields a correlation of 0.42/0.53/0.34 between the true diameter and the first component, respectively.

Altogether, our proposed estimator is fully data-driven, fast even for large sample sizes, automatically positive definite and can handle certain long-memory processes. The protein data example and further simulations in the Supplementary Material suggest that our approach yields robust estimators even when data are not normally distributed. In contrast, the tapering estimator is not data-driven in all data scenarios and must be manipulated to become positive definite. To the best of our knowledge, the tapering estimator has been not studied for non-Gaussian data. Our method is implemented in the R package `vstdct`.

A Appendix

Throughout the appendix, we denote by c, c_1, C, C_1, \dots etc. generic constants, that are independent of n and p . To simplify the notation, the constants are sometimes skipped and we write \lesssim for less than or equal to up to constants.

A.1 Proof of Lemma 1

We embed the p -dimensional Toeplitz matrix $\Sigma = \text{toep}(\sigma_0, \dots, \sigma_{p-1})$ in a $(2p-2)$ -dimensional circulant matrix $\tilde{\Sigma} = \text{toep}(\sigma_0, \dots, \sigma_{p-1}, \sigma_{p-2}, \dots, \sigma_1)$. Then, $\tilde{\Sigma} = U\Lambda U^*$, where $U = (2p-2)^{-1/2}[\exp\{\pi i(k-1)(l-1)/(p-1)\}]_{k,l=1}^{2p-2}$ with the conjugate transpose U^* , and Λ is a diagonal matrix with the k th diagonal value for $k = 1, \dots, p$ given by

$$\lambda_k = \sum_{l=1}^p \sigma_{l-1} \exp\{\pi i x_k (l-1)\} + \sum_{l=p+1}^{2p-2} \sigma_{2p-1-l} \exp\{\pi i x_k (l-1)\},$$

where $x_k = (k-1)/(p-1)$. By symmetry, $\lambda_k = \lambda_{2p-k}$ for $k = p+1, \dots, 2p-2$. Furthermore, $\Sigma = V^* \Lambda V$, where $V \in \mathbb{C}^{(2p-2) \times p}$ contains the first p columns of U . Then, for $i, j = 1, \dots, p$,

$$(D\Sigma D)_{i,j} = (DV^* \Lambda V D)_{i,j} = \sum_{r=1}^{2p-2} \lambda_r \sum_{q=1}^p D_{iq} V_{qr}^* \sum_{s=1}^p V_{rs} D_{sj}.$$

Define the scaling factor $a_s = 2^{-1/2}$ for $s = 1, p$ and $a_s = 1$ for $s = 2, \dots, p-2$, appearing in the definition of the discrete cosine transform I matrix. Then,

$$\begin{aligned} \sum_{s=1}^p V_{rs} D_{sj} &= (p-1)^{-1} \sum_{s=1}^p a_s a_j \exp\{\pi i (r-1)x_s\} \cos\{\pi(j-1)x_s\} \\ &\quad \pm \frac{a_j}{p-1} \exp(0) \cos(0) \pm \frac{a_j}{p-1} \exp\{\pi i (r-1)\} \cos\{\pi(j-1)\} \\ &= a_j \frac{2^{1/2} - 2}{p-1} \mathbb{1}_{\{|j-r| \text{ even}\}} + \frac{a_j}{p-1} \sum_{s=1}^p \exp\{\pi i (r-1)x_s\} \cos\{\pi(j-1)x_s\} \\ &= a_j b(j, r) + a_j ic(j, r), \end{aligned}$$

where $\mathbb{1}$ is the indicator function and

$$b(j, r) = \frac{2^{1/2} - 2}{p-1} \mathbb{1}_{\{|j-r| \text{ even}\}} + \frac{1}{p-1} \sum_{s=1}^p \cos\{\pi(r-1)x_s\} \cos\{\pi(j-1)x_s\},$$

$$c(j, r) = \frac{1}{p-1} \sum_{s=1}^p \sin\{\pi(r-1)x_s\} \cos\{\pi(j-1)x_s\}.$$

By the symmetry properties of cosine and sine, $b(j, r) = b(j, 2p-r)$ and $c(j, r) = -c(j, 2p-r)$ for $r = p+1, \dots, 2p-2$. Using $(\sum_{s=1}^p V_{rs} D_{sj})^* = \sum_{q=1}^p D_{jq} V_{qr}^*$, we obtain

$$(D\Sigma D)_{i,j} = \begin{cases} a_j^2 \sum_{r=1}^{2p-2} \lambda_r \{b(j, r)^2 + c(j, r)^2\}, & i = j \\ a_i a_j \sum_{r=1}^{2p-2} \lambda_r (b(i, r) + ic(i, r))(b(j, r) - ic(j, r)), & i \neq j. \end{cases} \quad (\text{A.1})$$

Some calculations show, for $r = 1, \dots, p$, that

$$\frac{1}{p-1} \sum_{s=1}^p \cos\{\pi(r-1)x_s\} \cos\{\pi(j-1)x_s\} = \begin{cases} \frac{1}{p-1}, & r \neq j, r-j \text{ even} \\ 0, & r-j \text{ odd} \\ \frac{p+1}{2p-2}, & r = j \neq 1, p \\ \frac{p}{p-1}, & r = j = 1, p \end{cases} \quad (\text{A.2})$$

$$\begin{aligned} & \frac{1}{p-1} \sum_{s=1}^p \sin\{\pi(r-1)x_s\} \cos\{\pi(j-1)x_s\} \\ &= \frac{\{1 - (-1)^{r-j}\}}{4(p-1)} [\cot\{\pi(r-j)/(2p-2)\} + \cot\{\pi(j+r-2)/(2p-2)\}]. \end{aligned} \quad (\text{A.3})$$

Using the Taylor expansion of the cotangens, i.e., $\cot(x) = x^{-1} - x/3 - x^3/45 + \dots$, for $0 < |x| < \pi$, one obtains for $r = 1, \dots, p$

$$c(j, r) = \frac{(r-1)\{1 - (-1)^{r-j}\}}{\pi\{(r-1) - (j-1)\}\{(r-1) + (j-1)\}} + \mathcal{O}\left\{\frac{2\pi(2r-2)}{3(2p-2)^2}\right\}, \quad (\text{A.4})$$

where the \mathcal{O} term does not depend on j and the constant does not depend on r, p .

Case $i = j$

The equations (A.1) – (A.3) imply

$$\begin{aligned}
(\mathbf{D}\Sigma\mathbf{D})_{j,j} &= a_j^2 \sum_{\substack{r=1 \\ r \neq j, \\ r \neq 2p-j}}^{2p-2} \lambda_r \left[\frac{(2^{1/2} - 2)^2 + 1 + 2(2^{1/2} - 2)(p-1)}{(p-1)^2} \mathbb{1}_{\{|r-j| \text{ even}\}} + c(j,r)^2 \right] \\
&\quad + a_j^2 \lambda_j \cdot \begin{cases} 2 \left(\frac{2^{1/2}-2}{p-1} + \frac{p+1}{2p-2} \right)^2, & j \neq 1, p \\ \left(\frac{2^{1/2}-2}{p-1} + \frac{p}{p-1} \right)^2, & j = 1, p \end{cases} \\
&= a_j^2 \sum_{\substack{r=1 \\ r \neq j, \\ r \neq 2p-j}}^{2p-2} \lambda_r \left[\frac{(2^{1/2} - 1)^2}{(p-1)^2} \mathbb{1}_{\{|r-j| \text{ even}\}} + c(j,r)^2 \right] + \lambda_j \cdot \begin{cases} \frac{2(2^{1/2}-3/2+p/2)^2}{(p-1)^2}, & j \neq 1, p \\ \frac{(2^{1/2}-2+p)^2}{2(p-1)^2}, & j = 1, p \end{cases} \\
&= \mathcal{O}(p^{-1}) + 2a_j^2 \sum_{r=1}^{p-1} \lambda_r c(j,r)^2 + \lambda_j \{0.5 + \mathcal{O}(p^{-1})\},
\end{aligned}$$

where we used the symmetry properties of λ_r and that by assumption $\|f\| < M_0$. Note that the \mathcal{O} terms do not depend on j . Since the complex exponential function is Lipschitz continuous with Lipschitz constant $L = 1$, it holds $\lambda_r = \lambda_j + L_{r,j}|r - j|(p-1)^{-1}$ where $-1 \leq L_{r,j} \leq 1$ is a constant depending on r, j . Then,

$$\sum_{r=1}^{p-1} \lambda_r c(j,r)^2 = \lambda_j \sum_{r=1}^{p-1} c(j,r)^2 + p^{-1} \sum_{r=1}^{p-1} L_{r,j} |r-j| c(r,j)^2.$$

Since $\sum_{r=1}^{p-1} \lambda_r c(1,r)^2 = -\sum_{r=1}^{p-1} \lambda_r c(p,r)^2$, it is sufficient to consider $j = 1, \dots, p-1$. We begin with first sum. For a shorter notation, we use $k = r-1$ and $l = j-1$ in the following. Then, summing the squares of the first term in (A.4) for $l = 0, \dots, p-2$ yields

$$\frac{1}{\pi^2} \sum_{k=0}^{p-2} \frac{k^2 \{1 - (-1)^{k-l}\}^2}{(k-l)^2 (k+l)^2} = \frac{4}{\pi^2} \begin{cases} \sum_{x=1}^{\infty} \frac{1}{(2x-1)^2} - R_1(l,p) = \frac{\pi^2}{8} - R_1(l,p), & l = 0 \\ \sum_{x=1}^{\infty} \frac{(2x)^2}{(2x-l)^2 (2x+l)^2} - R_2(l,p) = \frac{\pi^2}{16} - R_2(l,p), & l \text{ odd} \\ \sum_{x=1}^{\infty} \frac{(2x-1)^2}{(2x-1-l)^2 (2x-1+l)^2} - R_2(l,p) = \frac{\pi^2}{16} - R_3(l,p), & \text{else} \end{cases}$$

see Chapter 23.2 of Abramowitz and Stegun (1964) on sums of reciprocal powers.

If p is even, then the residual terms are given by

$$R_1(l,p) = \sum_{x=(p-2)/2}^{\infty} \frac{1}{(2x-1)^2} = \frac{\phi^{(1)}\{(p-3)/2\}}{4},$$

$$\begin{aligned}
R_2(l, p) &= \sum_{x=p/2}^{\infty} \frac{(2x)^2}{(2x-l)^2(2x+l)^2} \\
&= \frac{2\phi\{(p+l)/2\} - 2\phi\{(p-l)/2\} + l[\phi^{(1)}\{(p+l)/2\} + \phi^{(1)}\{(p-l)/2\}]}{16l}, \\
R_3(l, p) &= \sum_{x=p/2}^{\infty} \frac{(2x-1)^2}{(2x-1-l)^2(2x-1+l)^2} \\
&= \frac{2\phi\{(p-1+l)/2\} - 2\phi\{(p-1-l)/2\} + l[\phi^{(1)}\{(p-1+l)/2\} + \phi^{(1)}\{(p-1-l)/2\}]}{16l},
\end{aligned}$$

where ϕ and $\phi^{(1)}$ denote the digamma function and its derivative. If p is odd, similar remainder terms can be derived. To see that $R_i(l, p) = \mathcal{O}(p^{-1})$ for $i = 1, 2, 3$ and uniformly in l we use that asymptotically $\phi(x) \sim \log(x) - 1/(2x)$ and $\phi^{(1)}(x) \sim 1/x + 1/(2x^2)$. The mixed term $4/3 \sum_{k=0}^{p-2} \frac{k^2 \{1 - (-1)^{k-l}\}^2}{(k-l)(k+l)(2p-2)^2}$ and the squared \mathcal{O} term $16\pi^2/9 \sum_{k=0}^{p-2} \frac{k^2}{(2p-2)^4}$ are both of the order p^{-1} . Furthermore,

$$\frac{1}{p-1} \sum_{r=1}^{p-1} L_{r,j} |r-j| c(r, j)^2 = \frac{1}{p-1} \sum_{k=0}^{p-2} \frac{k^2 \{1 - (-1)^{k-l}\}^2 L_{k,l} |k-l|}{\pi^2 (k-l)^2 (k+l)^2} = \mathcal{O}\{p^{-1} \log p\},$$

since the harmonic sum diverges at a rate of $\log p$. Finally, $\lambda_j = f(x_j) + \mathcal{O}\{p^{-\beta} \log p\}$ by the uniform approximation properties of the discrete Fourier series for Hölder continuous functions (Zygmund, 2002). All together, we have shown that $(D\Sigma D)_{j,j} = f(x_j) + \mathcal{O}\{p^{-1} + p^{-\beta} \log p\}$, where the \mathcal{O} terms are uniform over $j = 1, \dots, p$.

Case $i \neq j$ and $|i-j|$ is even

In this case, $(D\Sigma D)_{i,j} = a_i a_j \sum_{r=1}^{2p-2} \lambda_r \{b(i, r)b(j, r) + c(i, r)c(j, r)\}$ since $|r-j|$, and $|r-i|$ are both either odd or even. Note that $b(i, r)b(j, r) = \mathcal{O}(p^{-2})$ for $r \neq i, j$ and $b(i, r)b(j, r) = \mathcal{O}(p^{-1})$ if $i = r$ or $j = r$, where the $\mathcal{O}(\cdot)$ terms are uniformly in i, j . Since $b(i, r) \geq 0$ and $\|f\|_{\infty} < M_0$, it follows $a_i a_j \sum_{r=1}^{2p-2} \lambda_r b(i, r)b(j, r) = \mathcal{O}(p^{-1})$ uniformly in i, j . We proceed similarly as before to show that $a_i a_j \sum_{r=1}^{2p-2} \lambda_r c(i, r)c(j, r) = \mathcal{O}(p^{-1})$. Setting $k = r-1$, $l = j-1$, $m = i-1$ and using that $l \neq m$ and $|l-m|$ is even, one obtains

$$\frac{1}{\pi^2} \sum_{k=0}^{p-2} \frac{k^2 \{1 - (-1)^{k-l}\} \{(-1)^{k-m} - 1\}}{(k-l)(k+l)(k-m)(k+m)}$$

$$= \frac{4}{\pi^2} \begin{cases} \sum_{x=1}^{\infty} \frac{(2x)^2}{(2x-l)(2x+l)(2x-m)(2x+m)} - R_1(l, m, p) = -R_1(l, m, p), & l, m \text{ odd} \\ \sum_{x=1}^{\infty} \frac{(2x-1)^2}{(2x-1-l)(2x-1+l)(2x-1-m)(2x-1+m)} - R_2(l, m, p) = -R_2(l, m, p), & l, m \text{ even,} \end{cases}$$

where for even p the residual terms are given by

$$R_1(l, m, p) = \sum_{x=p/2}^{\infty} \frac{(2x)^2}{(2x-l)(2x+l)(2x-m)(2x+m)}$$

$$R_2(l, m, p) = \sum_{x=p/2}^{\infty} \frac{(2x-1)^2}{(2x-1-l)(2x-1+l)(2x-1-m)(2x-1+m)}.$$

Similarly as before, one can show that $R_1(l, m, p)$ and $R_2(l, m, p)$ are of the order $\mathcal{O}(p^{-1})$ where the hidden constant does not depend on l, m . If p is odd, analogous residual terms can be derived. Using similar techniques as before, one can show that the two residual terms and the remaining mixed and square terms vanish at a rate of the order $\mathcal{O}(p^{-1})$ and uniformly in i, j .

Case $i \neq j$ and $|i - j|$ is odd

$|r - i|$ and $|r - j|$ are either odd and even, or even and odd. Without loss of generality, assume that $|r - i|$ is even. Then, $(D\Sigma D)_{i,j} = a_i a_j \sum_{r=1}^{2p-2} \lambda_r b(i, r) c(j, r)$. Since $b(i, \cdot)$ is an even function, $c(j, \cdot)$ is an odd function and $\lambda_r = \lambda_{2p-r}$, it follows $(D\Sigma D)_{i,j} = 0$. \square

A.2 Periodic Smoothing Splines

In this section we recapitulate the results obtained in Schwarz and Krivobokova (2016) for the equivalent kernels of periodic smoothing spline estimators. Given data points $\{(x_i, Y_i)\}_{i=1}^N$ with true relationship $Y_i = f(x_i) + \epsilon_i$, where $x_i = i/N$ and the residuals ϵ_i satisfy standard assumptions, the periodic smoothing spline estimator \hat{f} is the solution to

$$\min_{s \in S_{\text{per}}(2q-1, \underline{x}_N)} \left[\frac{1}{N} \sum_{i=1}^N \{Y_i - s(x_i)\}^2 + h^{2q} \int_0^1 \{s^{(q)}(x)\}^2 dx \right],$$

where $h > 0$ is the smoothing parameter, $q \in \mathbb{N}$ the penalty order and $S_{\text{per}}(2q-1, \underline{x}_N)$ the periodic spline space of degree $2q - 1$ based on knots $\underline{x}_N = (x_i)_{i=0}^N = (i/N)_{i=0}^N$. Schwarz and Krivobokova (2016) have shown that $\hat{f}(x) = N^{-1} \sum_{i=1}^N W(x, x_i) Y_i$, where $W(x, x_i)$ is known as effective kernel of a periodic smoothing spline estimator and its explicit expression is

$$W(x, x_i) = \sum_{j=1}^N \frac{\Phi\{Nx + q, \exp(-2\pi i j/N)\} \overline{\Phi\{Nx_i + q, \exp(-2\pi i j/N)\}}}{Q_{2q-2}(j/N) + h^{2q}(2\pi j)^{2q} \text{sinc}(\pi j/N)^{2q}},$$

where $\Phi(\cdot, \cdot)$ denotes exponential splines (Schoenberg, 1973) with complex conjugate $\overline{\Phi(\cdot, \cdot)}$. The polynomials $Q_{2q-2}(x)$ are formally defined as $Q_{2q-2} = \sum_{l=-\infty}^{\infty} \text{sinc}\{\pi(x+l)\}^{2q}$; for the explicit expressions see Section 4.1.1 in Schwarz (2012). A scaled version $K(x, t)$ of $W(x, t)$ in terms of the bandwidth parameter h is defined as $K(x, t) = hW(hx, ht)$. We denote by $K_h(x, t) = K(x/h, t/h) = hW(x, t)$. Also, we use that $W(x, t) = \sum_{l=-\infty}^{\infty} \mathcal{W}(x, t+l)$ (see Lemma 14 in Schwarz, 2012), where

$$\mathcal{W}(x, t) = \int_0^N \frac{\Phi\{Nx + q, \exp(-2\pi i u)\} \overline{\Phi\{Nx_i + q, \exp(-2\pi i u)\}}}{Q_{2q-2}(u) + h^{2q}(2\pi j)^{2q} \text{sinc}(\pi u)^{2q}} du$$

is the asymptotic equivalent kernel of smoothing spline estimators on \mathbb{R} . Finally, we denote $\mathcal{K}_h(x, t) = \mathcal{K}(x/h, t/h) = h\mathcal{W}(x, t)$.

A.3 Proof of Theorem 1

The structure of the proof is as follows. First, we derive the L_∞ rate of the periodic smoothing spline estimator $\widehat{H}(f)$. Then, using the Cauchy-Schwarz inequality and a mean value argument, the convergence rate of the spectral density estimator \hat{f} is established. With the relationship $E\|\widehat{\Sigma} - \Sigma\| \leq E\|\hat{f} - f\|_\infty^2$ the first claim of the theorem follows. Finally, we prove the second statement on the precision matrices. For the sake of clarity, the proof of the auxiliary Lemmas 2, 3 and 4 are listed separately in Section B.

A.3.1 An upper bound on $E\|\widehat{H}(f) - H(f)\|_\infty^2$

Proposition 1. *Let $\Sigma = \Sigma(f)$ with $f \in \mathcal{F}_\beta$ such that $\beta > 0$. If $h > 0$ such that $h \rightarrow 0$ and $hT \rightarrow \infty$, then with $T = \lfloor p^v \rfloor$ for any $v \in (1 - \min\{1, \beta\}/3, 1)$, the estimator $\widehat{H}(f)$ described in Section 3 with $q = \max\{1, \gamma\}$ satisfies for $p \rightarrow \infty$ and n such that $p^{\min\{1, \beta\}}/n \rightarrow c \in (0, \infty]$*

$$E\|\widehat{H}(f) - H(f)\|_\infty^2 = \mathcal{O}\{\log(np)/(nph)\} + \mathcal{O}(h^{2\beta}).$$

Proof. Application of the triangle inequality yields a bias-variance decomposition

$$E\|\widehat{H}(f) - H(f)\|_\infty^2 \leq 2E\|\widehat{H}(f) - E\{\widehat{H}(f)\}\|_\infty^2 + 2\|E\{\widehat{H}(f)\} - H(f)\|_\infty^2. \quad (\text{A.5})$$

Set $\tilde{T} = 2T - 2$ and $x_k = (k - 1)/\tilde{T}$ for $k = 1, \dots, \tilde{T}$. The periodic smoothing spline estimator $\widehat{H}(f)$ can be represented as a kernel estimator with respect to a kernel function $W(x, y)$ or the scaled version $K_h(x, t) = hW(x, t)$. An explicit representation of the kernel is derived in (Schwarz and Krivobokova, 2016). A summary of their results is given in the Appendix A.2. Lemma 4 listed in the Section B gives the following decomposition of $\widehat{H}(f)(x)$ for $x \in [0, 1]$ into a deterministic, a Gaussian, and a non-Gaussian part

$$\widehat{H}(f)(x) = \frac{1}{\tilde{T}} \sum_{k=1}^{\tilde{T}} W(x, x_k) Y_k^* = \frac{1}{\tilde{T}h} \sum_{k=1}^{\tilde{T}} K_h(x, x_k) [H\{f(x_k)\} + \epsilon_k + \zeta_k + \xi_k],$$

where $|\epsilon_k| \lesssim (np)^{-1} + (np)^{-\beta} \log p$, $\zeta_k \sim \mathcal{N}(0, m^{-1})$ with $\text{cov}(\zeta_k, \zeta_l) = \mathcal{O}\{p^{-2} + p^{-2\beta}(\log p)^2\}$ for $k \neq l$. The random variable ξ_k satisfies $E|\xi_k|^\ell \lesssim (\log m)^{2\ell}\{m^{-\ell} + (T^{-1} + T^{-1}p^{1-\beta} \log p)^\ell\}$ for each integer $\ell > 1$ and has mean zero. Mirroring and reenumerating $\zeta_k, \eta_k, \epsilon_k$ is similar as for Y_k^* ($k = 1, \dots, \tilde{T}$).

Upper bound on the variance

Using the above representation, one can write

$$E\|\widehat{H}(f) - E\{\widehat{H}(f)\}\|_\infty^2 = E \left\| \frac{1}{\tilde{T}} \sum_{k=1}^{\tilde{T}} W(x, x_k) (\zeta_k + \xi_k) \right\|_\infty^2. \quad (\text{A.6})$$

First, we bound the supremum by a maximum over a finite number of points. If $q > 1$, then $W(\cdot, x_k)$ is Lipschitz continuous with constant $L > 0$. In this case, it holds almost surely that

$$\begin{aligned} & \sup_{x \in [0,1]} \left| \frac{1}{\tilde{T}} \sum_{k=1}^{\tilde{T}} W(x, x_k) (\zeta_k + \xi_k) \right|^2 \\ & \leq \left[\max_{1 \leq j \leq \tilde{T}} \left| \frac{1}{\tilde{T}} \sum_{k=1}^{\tilde{T}} W(x_j, x_k) (\zeta_k + \xi_k) \right| + \sup_{\substack{x, x' \in [0,1], \\ |x-x'| < 1/\tilde{T}}} \left| \frac{1}{\tilde{T}} \sum_{k=1}^{\tilde{T}} \{W(x, x_k) - W(x', x_k)\} (\zeta_k + \xi_k) \right| \right]^2 \\ & \leq 2 \max_{1 \leq j \leq \tilde{T}} \left| \frac{1}{\tilde{T}} \sum_{k=1}^{\tilde{T}} W(x_j, x_k) (\zeta_k + \xi_k) \right|^2 + \frac{2L^2}{\tilde{T}^4} \left(\sum_{k=1}^{\tilde{T}} |\zeta_k + \xi_k| \right)^2. \end{aligned}$$

Using $E\{(\sum_{k=1}^{\tilde{T}} |\zeta_k + \xi_k|)^2\} \lesssim E\{(\sum_{k=1}^{\tilde{T}} |\zeta_k|)^2\} + E\{(\sum_{k=1}^{\tilde{T}} |\xi_k|)^2\} \lesssim \tilde{T}^2 m^{-1}$, one gets

$$(A.6) \lesssim E \left\{ \max_{1 \leq j \leq \tilde{T}} \left| \frac{1}{\tilde{T}} \sum_{k=1}^{\tilde{T}} W(x_j, x_k) (\zeta_k + \xi_k) \right|^2 \right\} + o\{(np)^{-1}\}. \quad (A.7)$$

If $q = 1$, then $\sum_{k=1}^{\tilde{T}} W(\cdot, x_k)$ is a piecewise linear function with knots at $x_j = j/\tilde{T}$. The factor $(\zeta_k + \xi_k)$ can be considered as stochastic weights that do not affect the piecewise linear property. Thus, the supremum is attained at one of the knots $x_j = j/\tilde{T}$ for $j = 1, \dots, \tilde{T}$, and (A.7) is also valid for $q = 1$. Again with $(a+b)^2 \leq 2a^2 + 2b^2$ we obtain

$$(A.6) \lesssim E \left\{ \max_{1 \leq j \leq \tilde{T}} \left| \frac{1}{\tilde{T}} \sum_{k=1}^{\tilde{T}} W(x_j, x_k) \zeta_k \right|^2 \right\} + E \left\{ \max_{1 \leq j \leq \tilde{T}} \left| \frac{1}{\tilde{T}} \sum_{k=1}^{\tilde{T}} W(x_j, x_k) \xi_k \right|^2 \right\} + o\{(np)^{-1}\}.$$

We start with bounding $T_1 = E\{\max_{1 \leq j \leq \tilde{T}} |(\tilde{T}h)^{-1} \sum_{k=1}^{\tilde{T}} K_h(x_j, x_k) \zeta_k|^2\}$ with Lemma 1.6 of Tsybakov (2009). This requires a bound on $\|(\tilde{T}h)^{-1} \sum_{k=1}^{\tilde{T}} K_h(x_j, x_k) \zeta_k\|_{\psi_2}^2$ where $\|\cdot\|_{\psi_2}$ denotes the sub-Gaussian norm. In case of a Gaussian random variable the norm equals to the variance. See (Vershynin, 2018) for further details on the sub-Gaussian distribution.

Using the properties of the kernel function K_h stated in Lemma 2 of the Supplementary Material, we obtain

$$\begin{aligned} & \left\| \frac{1}{\tilde{T}h} \sum_{k=1}^{\tilde{T}} K_h(x_j, x_k) \zeta_k \right\|_{\psi_2}^2 = \text{var} \left\{ \frac{1}{\tilde{T}h} \sum_{k=1}^{\tilde{T}} K_h(x_j, x_k) \zeta_k \right\} \\ & = \frac{1}{\tilde{T}^2 h^2} \sum_{k=1}^{\tilde{T}} K_h(x_j, x_k)^2 \text{var}(\zeta_k) + \frac{1}{\tilde{T}^2 h^2} \sum_{k=1}^{\tilde{T}} K_h(x_j, x_k) \sum_{l=1}^{\tilde{T}} K_h(x_j, x_l) \text{cov}(\zeta_k, \zeta_l) \\ & \leq C(Thm)^{-1} + C' \{p^{-2} + p^{-2\beta} (\log p)^2\}. \end{aligned}$$

Lemma 1.6 of (Tsybakov, 2009) then yields

$$T_1 \lesssim \log(2\tilde{T}) [C(Thm)^{-1} + C' \{p^{-2} + (\log p)^2 p^{-2\beta}\}] = \mathcal{O}\{(Thm)^{-1} \log(2\tilde{T}) + h^{2\beta}\}. \quad (\text{A.8})$$

To see this, note that $p^{\min\{1, \beta\}}/n \rightarrow c \in (0, \infty]$ implies $p^{-1} = \mathcal{O}(n^{-1})$. Thus, if $\beta > 1$, then

$$\log(2\tilde{T}) \{p^{-2} + p^{-2\beta} (\log p)^2\} \lesssim \log(2\tilde{T}) p^{-2} \lesssim \log(2\tilde{T}) (Tm)^{-1}.$$

Now consider $0 < \beta \leq 1$. Recall that $T = \lfloor p^v \rfloor$ for some fixed $v \in (1 - \min\{1, \beta\}/3, 1)$. One can find a constant $a = C_v$ depending on v but not on n, p such that the inequality $\log(x) \leq x^a/a$ implies $\log(2\tilde{T}) \log(p)^2 p^{-2\beta} T^{2\beta} = \mathcal{O}(1)$. Thus, $\log(2\tilde{T}) \log(p)^2 p^{-2\beta} = \mathcal{O}(h^{2\beta})$ since $hT \rightarrow \infty$ by assumption.

Next, we derive a bound for the second term $T_2 = E\{\max_{1 \leq j \leq \tilde{T}} |(\tilde{T}h)^{-1} \sum_{k=1}^{\tilde{T}} K_h(x_j, x_k) \xi_k|^2\}$. The exponential decay property of the kernel K_h , see Lemma 2 in the Section B, yields

$$T_2 \lesssim E \left\{ \max_{1 \leq j \leq \tilde{T}} \left| \frac{1}{\tilde{T}h} \sum_{k=1}^{\tilde{T}} \gamma_h(x_j, x_k) |\xi_k| \right|^2 \right\},$$

where $\gamma_h(x, t) = \gamma^{|x-t|/h} + \gamma^{1/h} \{\gamma^{(x-t)/h} + \gamma^{(t-x)/h}\} (1 - \gamma^{1/h})^{-1}$ and $\gamma \in (0, 1)$ is a constant. For some threshold $R > 0$ specified later, define $\xi_k^- = |\xi_k| \mathbb{1}\{|\xi_k| \leq R\}$ and

$\xi_k^+ = |\xi_k| \mathbb{1}\{|\xi_k| > R\}$. Then,

$$T_2 \lesssim E \left\{ \max_{1 \leq j \leq \tilde{T}} \left| \frac{1}{\tilde{T}h} \sum_{k=1}^{\tilde{T}} \gamma_h(x_j, x_k) \xi_k^- \right|^2 \right\} + E \left\{ \max_{1 \leq j \leq \tilde{T}} \left| \frac{1}{\tilde{T}h} \sum_{k=1}^{\tilde{T}} \gamma_h(x_j, x_k) \xi_k^+ \right|^2 \right\}. \quad (\text{A.9})$$

The first term in (A.9) can be bounded again with Lemma 1.6 of Tsybakov (2009). We use the fact that for not necessarily independent random variables X_1, \dots, X_N with $|X_i| < R$ ($i = 1, \dots, N$) it holds $\|\sum_{i=1}^N a_i X_i\|_{\psi_2}^2 \leq 4R^2 \sum_{i=1}^N a_i^2$ where $a_1, \dots, a_N \in \mathbb{R}$ and $R > 0$ are constants. This is a consequence of Lemma 1 of Azuma (1967) which yields $E\{\exp(\lambda \sum_{i=1}^N a_i X_i)\} \leq \exp(\lambda^2 R^2 \sum_{i=1}^N a_i^2)$ for all $\lambda \in \mathbb{R}$. Thus, for all $t > 0$ holds $\text{pr}(|\sum_{i=1}^N a_i X_i| > t) \leq 2 \exp(-\lambda t + \lambda^2 R^2 \sum_{i=1}^N a_i^2)$. Setting $\lambda = t/2 \cdot (R^2 \sum_{i=1}^N a_i^2)^{-1}$, it follows that $\sum_{i=1}^N a_i X_i$ has a sub-Gaussian distribution and the sub-Gaussian norm is bounded by $2R(\sum_{i=1}^N a_i^2)^{1/2}$.

Together, we get $\|(\tilde{T}h)^{-1} \sum_{k=1}^{\tilde{T}} \gamma_h(x_j, x_k) \xi_k^-\|_{\psi_2}^2 \leq 4R^2 (\tilde{T}h)^{-2} \sum_{k=1}^{\tilde{T}} \gamma_h(x_j, x_k)^2 \lesssim R^2 (\tilde{T}h)^{-1}$, where we used the bound on γ_h from Lemma 2. Applying Lemma 1.6 of Tsybakov (2009) then yields

$$E \left\{ \max_{1 \leq j \leq \tilde{T}} \left| \frac{1}{\tilde{T}h} \sum_{k=1}^{\tilde{T}} \gamma_h(x_j, x_k) \xi_k^- \right|^2 \right\} \lesssim \frac{R^2}{\tilde{T}h} \log(2\tilde{T}). \quad (\text{A.10})$$

To bound the second term in (A.9), we use the moment bounds for ξ_k derived in Lemma 4. Then, for all integers $\ell > 1$

$$\begin{aligned} E \left\{ \max_{1 \leq j \leq \tilde{T}} \left| \frac{1}{\tilde{T}h} \sum_{k=1}^{\tilde{T}} \gamma_h(x_j, x_k) \xi_k^+ \right|^2 \right\} &= E \left\{ \max_{1 \leq j \leq \tilde{T}} \left| \frac{1}{\tilde{T}h} \sum_{k=1}^{\tilde{T}} \gamma_h(x_j, x_k) (\xi_k^+)^{\ell} (\xi_k^+)^{1-\ell} \right|^2 \right\} \\ &\leq R^{2-2\ell} E \left\{ \max_{1 \leq j \leq \tilde{T}} \frac{1}{\tilde{T}^2 h^2} \sum_{k=1}^{\tilde{T}} \gamma_h(x_j, x_k)^2 \cdot \sum_{k=1}^{\tilde{T}} (\xi_k^+)^{2\ell} \right\} \leq R^{2-2\ell} E \left(\frac{C_1}{\tilde{T}h} \sum_{k=1}^{\tilde{T}} \xi_k^{2\ell} \right) \\ &\lesssim h^{-1} R^{2-2\ell} (\log m)^{4\ell} \{m^{-2\ell} + (T^{-1} + T^{-1} p^{1-\beta} \log p)^{2\ell}\}. \end{aligned} \quad (\text{A.11})$$

Combining the error bounds (A.10) and (A.11) and choosing $R = m^{-1/2}$ gives

$$T_2 \lesssim \frac{\log T}{mTh} + \frac{(\log m)^{4\ell}}{hm^{1-\ell}} \cdot \begin{cases} \frac{(\log p)^{2\ell} p^{2\ell(1-\beta)}}{T^{2\ell}} + m^{-2\ell}, & 0 < \beta \leq 1, \\ T^{-2\ell} + m^{-2\ell}, & 1 < \beta. \end{cases}$$

By assumption $T = \lfloor p^v \rfloor$ and $m = \lfloor np^{(1-v)} \rfloor$ for some fixed $v \in (1 - \min\{1, \beta\}/3, 1)$. If ℓ is an integer such that $\ell \geq 1/(1-v)$, then

$$m^{\ell-1}(\log m)^{4\ell} m^{-2\ell} \lesssim m^{-\ell} \lesssim n^{-\ell} p^{-(1-v)\ell} = \mathcal{O}\{(np)^{-1}\},$$

where we used $\log x \leq x^a/a$ with $a = 1/(4\ell)$. Now, consider $0 < \beta \leq 1$. Then, $n \leq cp^\beta$ by assumption. Let $0 < \chi < 1$ be a small constant. Using the inequality $\log x \leq x^a/a$ twice with $a = \chi/(2\ell)$ gives

$$\begin{aligned} m^{\ell-1}(\log m)^{4\ell}(\log p)^{2\ell} p^{2\ell(1-\beta)} T^{-2\ell} &\lesssim n^{\ell-1+\chi} p^{(1-v)(\ell-1+\chi)-2\ell v+2\ell(1-\beta)+\chi} \\ &\lesssim p^{\ell(3-3v-\beta)+(\beta+\chi+1)(1-v)+\chi}. \end{aligned} \quad (\text{A.12})$$

Note that for $v \in (1 - \beta/3, 1)$, the condition $\ell(3 - 3v - \beta) + (\beta + \chi + 1)(1 - v) + \chi < -2$ is equivalent to $\ell > \{-2 - (\beta + \chi + 1)(1 - v) - \chi\}/(3 - 3v - \beta)$. Thus, for any fixed v one can find an integer ℓ which is independent of n, p such that the right side of (A.12) is of the order $\mathcal{O}(p^{-2})$. For the same choice of ℓ it holds that $m^{\ell-1}(\log m)^{4\ell} T^{-2\ell} = \mathcal{O}(p^{-2})$.

In total, choosing an integer $\ell \geq \max[1/(1-v), \{-2 - (\beta + \chi + 1)(1 - v) - \chi\}/(3 - 3v - \beta)]$ gives

$$\mathbb{E}\|\widehat{H}(f) - \mathbb{E}\{\widehat{H}(f)\}\|_\infty^2 = \mathcal{O}\left\{\frac{\log(np)}{nph} + h^{2\beta}\right\}. \quad (\text{A.13})$$

Upper bound on the bias

Using the representation in Lemma 4 once more gives for each $x \in [0, 1]$

$$E\{\widehat{H}(f)(x)\} - H\{f(x)\} = \frac{1}{\tilde{T}h} \sum_{k=1}^{\tilde{T}} K_h(x, x_k) [H\{f(x_k)\} + \epsilon_k] - H\{f(x)\}.$$

The bounds on ϵ_k imply

$$\left| \frac{1}{\tilde{T}h} \sum_{k=1}^{\tilde{T}} K_h(x, x_k) \epsilon_k \right| \lesssim \frac{1}{\tilde{T}h} \sum_{k=1}^{\tilde{T}} \gamma_h(x_j, x_k) |\epsilon_k| \lesssim (np)^{-1} + (np)^{-\beta} \log p.$$

Consider the case that $\beta \geq 1$. In particular, $q = \gamma$ and $f^{(q)}$ is α -Hölder continuous. Since f is a periodic function with $f(x) \in [\delta, M_0]$ and $H(y) \propto \phi(m/2) + \log(2y/m)$, it follows that $\{H(f)\}^{(q)}$ is also α -Hölder continuous. Extending $g = H(f)$ to the entire real line, we get

$$\frac{1}{\tilde{T}h} \sum_{k=1}^{\tilde{T}} K_h(x, x_k) g(x_k) = \int_{-\infty}^{\infty} h^{-1} \mathcal{K}_h(x, t) g(t) dt + \mathcal{O}(\tilde{T}^{-\beta})$$

where \mathcal{K}_h is the extension of K_h to the entire real line (see Schwarz and Krivobokova, 2016). Expanding $g(t)$ in a Taylor series around x and using that $h^{-1} \mathcal{K}_h$ is a kernel of order $2q$, see Lemma 2(iii), it follows that for any $x \in [0, 1]$

$$\begin{aligned} \frac{1}{\tilde{T}h} \sum_{k=1}^{\tilde{T}} K_h(x, x_k) g(x_k) &= g(x) + \int_{-\infty}^{\infty} h^{-1} \mathcal{K}_h(x, t) (x-t)^q \frac{g^{(q)}(\xi_{x,t})}{q!} dt + \mathcal{O}(\tilde{T}^{-\beta}) \\ &= g(x) + \int_{-\infty}^{\infty} h^{-1} \mathcal{K}_h(x, t) (x-t)^q \frac{g^{(q)}(\xi_{x,t}) - g^{(q)}(x)}{q!} dt + \mathcal{O}(\tilde{T}^{-\beta}) \\ &= g(x) + \sum_{l=-\infty}^{\infty} \int_{x+(l-1)h}^{x+lh} \mathcal{K}_h(x, t) (x-t)^q \frac{g^{(q)}(\xi_{x,t}) - g^{(q)}(x)}{hq!} dt + \mathcal{O}(\tilde{T}^{-\beta}), \end{aligned}$$

where $\xi_{x,t}$ is a point between x and t . Using the fact that the kernel \mathcal{K}_h decays exponentially and that $g^{(q)}$ is α -Hölder continuous on $[\delta, M_0]$ with some constant L , one obtains

$$\begin{aligned} \left| \frac{1}{\tilde{T}h} \sum_{k=1}^{\tilde{T}} K_h(x, x_k) g(x_k) - g(x) \right| &\leq \frac{CL}{q!} \sum_{l=-\infty}^{\infty} \int_{x+(l-1)h}^{x+lh} \gamma^{\frac{|x-t|}{h}} |x-t|^q \frac{|\xi_{x,t} - x|^\alpha}{hq!} dt + \mathcal{O}(\tilde{T}^{-\beta}) \\ &\leq \frac{CL}{q!} \sum_{l=-\infty}^{\infty} \int_{x+(l-1)h}^{x+lh} \gamma^{\frac{|x-t|}{h}} \frac{|x-t|^\beta}{h} dt + \mathcal{O}(\tilde{T}^{-\beta}) \leq h^\beta \frac{CL}{q!} \sum_{l=-\infty}^{\infty} \gamma^{|l-1|} |l|^\beta + \mathcal{O}(\tilde{T}^{-\beta}) \\ &= \mathcal{O}(h^\beta) + \mathcal{O}(\tilde{T}^{-\beta}). \end{aligned}$$

If $0 < \beta \leq 1$, then $q = 1$ and g is β -Hölder continuous. Since $f(x) \in [\delta, M_0]$ and the logarithm is Lipschitz continuous on a compact interval, it follows $g = H(f)$ is

β -Hölder continuous. Expanding g to the entire line and using Lemma 2(iii) with $m = 0$ gives

$$\frac{1}{\tilde{T}h} \sum_{k=1}^{\tilde{T}} K_h(x, x_k) g(x_k) - g(x) = \int_{-\infty}^{\infty} \mathcal{K}_h(x, t) \frac{g(t) - g(x)}{h} dt + \mathcal{O}(\tilde{T}^{-\beta}).$$

In a similar way as before, one obtains

$$\left| \frac{1}{\tilde{T}h} \sum_{k=1}^{\tilde{T}} K_h(x, x_k) g(x_k) - g(x) \right| = \mathcal{O}(h^\beta) + \mathcal{O}(\tilde{T}^{-\beta}).$$

Note that $\tilde{T}^{-\beta} = o(h^\beta)$ as $hT \rightarrow \infty$ and $h \rightarrow 0$ by assumption. Since the derived bounds are uniform for $x \in [0, 1]$ it holds

$$\left\| E\{\widehat{H}(f)(x)\} - H\{f(x)\} \right\|_{\infty} = \mathcal{O}(h^\beta) + \mathcal{O}\{(np)^{-1} + (np)^{-\beta} \log p\}. \quad (\text{A.14})$$

Putting the bounds (A.13) and (A.14) together gives

$$E[\|\widehat{H}(f) - H(f)\|_{\infty}^2] = \mathcal{O}\{\log(np)/(nph)\} + \mathcal{O}(h^{2\beta}).$$

□

A.3.2 An upper bound on $E\|\hat{f} - f\|_{\infty}^2$

Proposition 2. *Let $\Sigma = \Sigma(f)$ with $f \in \mathcal{F}_\beta$ such that $\beta > 0$. If $h > 0$ such that $h \rightarrow 0$ and $hT \rightarrow \infty$, then with $T = \lfloor p^v \rfloor$ for any $v \in (1 - \min\{1, \beta\}/3, 1)$, the estimator \hat{f} described in Section 3 with $q = \max\{1, \gamma\}$ satisfies for $p \rightarrow \infty$ and n such that $p^{\min\{1, \beta\}}/n \rightarrow c \in (0, \infty]$*

$$E\|\hat{f} - f\|_{\infty}^2 = \mathcal{O}\{\log(np)/(nph)\} + \mathcal{O}(h^{2\beta}).$$

Proof. By the mean value theorem, it holds for some function g between $\widehat{H}(f)$ and $H(f)$ that

$$\begin{aligned} E\|\hat{f} - f\|_{\infty}^2 &= E\|H^{-1}\{\widehat{H}(f)\} - H^{-1}\{H(f)\}\|_{\infty}^2 = E\|(H^{-1})'(g)(\widehat{H}(f) - H(f))\|_{\infty}^2 \\ &\lesssim E\|H^{-1}(g)\{\widehat{H}(f) - H(f)\}\|_{\infty}^2. \end{aligned}$$

Application of the Cauchy-Schwarz inequality with a constant $C > 0$ yields

$$E\|\hat{f} - f\|_\infty^2 \leq C^2 E\|\widehat{H}(f) - H(f)\|_\infty^2 + (E\|\hat{f} - f\|_\infty^4)^{1/2} \cdot \text{pr}(\|H^{-1}(g)\|_\infty > C)^{1/2}. \quad (\text{A.15})$$

To show that the second term on the right-hand side of (A.15) is negligible, we use Markov's inequality. In order to do so, we first derive the asymptotic order of the moment generating function of $\widehat{H}(f)$ for $n, p \rightarrow \infty$.

Moment generating function of $\|\widehat{H}(f)\|_\infty$

By the exponential decay property of the kernel K stated in Lemma 2, it holds almost surely that

$$\|\widehat{H}(f)\|_\infty \lesssim \sup_{x \in [0,1]} \frac{1}{\tilde{T}h} \sum_{k=1}^{\tilde{T}} \gamma_h(x, x_k) \cdot |Y_k^*|,$$

where $\gamma_h(x, t) = \gamma^{|x-t|/h} + \gamma^{1/h} \{\gamma^{(x-t)/h} + \gamma^{(t-x)/h}\} / (1 - \gamma^{1/h})$ for some constant $\gamma \in (0, 1)$. First, $\|\widehat{H}(f)\|_\infty$ is bounded with the maximum over a finite number of points. Calculating the derivative of $s : [0, 1] \rightarrow \mathbb{R}$, $x \mapsto s(x) = \sum_{k=1}^{\tilde{T}} \gamma_h(x, x_k) |Y_k^*|$ for $x \neq x_k$ gives almost surely

$$\frac{\partial}{\partial x} s(x) = h^{-1} \log \gamma \sum_{k=1}^{\tilde{T}} \left[\gamma^{|x-x_k|/h} |x - x_k| + \frac{\gamma^{1/h}}{1 - \gamma^{1/h}} \{ \gamma^{(x-x_k)/h} + \gamma^{(x_k-x)/h} \} \right] |Y_k^*|.$$

Since $\partial s(x)/\partial x > 0$ almost surely for $x \neq x_k$, the extrema occur at x_k ($k = 1, \dots, \tilde{T}$). Thus, for $\lambda > 0$, the moment generating function of $\|\widehat{H}(f)\|_\infty$ is bounded, up to constants, by

$$E[\exp\{\lambda \|\widehat{H}(f)\|_\infty\}] \lesssim \sum_{j=1}^{\tilde{T}} E \left[\exp \left\{ \frac{\lambda}{\tilde{T}h} \sum_{k=1}^{\tilde{T}} \gamma_h(x_j, x_k) |Y_k^*| \right\} \right].$$

Let $M_j = (\tilde{T}h)^{-1} \sum_{k=1}^{\tilde{T}} \gamma_h(x_j, x_k)$, which by Lemma 2 is bounded uniformly in j by some global constant $M > 0$. By the convexity of the exponential function we

obtain

$$E \left[\exp \left\{ \frac{\lambda}{\tilde{T}h} \sum_{k=1}^{\tilde{T}} \gamma_h(x_j, x_k) |Y_k^*| \right\} \right] \leq \frac{1}{M_j \tilde{T}h} \sum_{k=1}^{\tilde{T}} \gamma_h(x_j, x_k) E[\exp\{\lambda M_j |Y_k^*|\}].$$

Recall that $Y_k^* = 2^{-1/2} \log(Q_k/m)$ and by assumption $0 \leq \delta \leq f \leq M_0$. Using Lemma 3, Q_k can be written as a sum of $m = np/T$ independent gamma random variables, i.e., $Q_k = \sum_{i=1}^m A_i$ where $A_i \sim \Gamma(1/2, 2a_i)$ with $a_i \in (c_1\delta, c_2M_0)$ for some constants $c_1, c_2 > 0$. Thus, we can find some (fully correlated) random variables $Q_k^- \sim \Gamma(m/2, \tilde{c}_1\delta)$ and $Q_k^+ \sim \Gamma(m/2, \tilde{c}_2M_0)$ such that $Q_k^- \leq Q_k \leq Q_k^+$ almost surely and $\tilde{c}_1, \tilde{c}_2 > 0$ are some constants. Then,

$$E[\exp\{\lambda M_j |Y_k^*|\}] \leq E[\exp\{\lambda M_j 2^{-1/2} \max\{|\log(Q_k^+/m)|, |\log(Q_k^-/m)|\}\}].$$

The moment generating function of $|\log X|$ with $X \sim \Gamma(a, b)$ is

$$E\{\exp(t|\log X|)\} = b^{-t} \frac{\Gamma(a-t) - \gamma(a-t, 1/b) + b^{2t} \gamma(a+t, 1/b)}{\Gamma(a)}, \quad |t| < a,$$

where $\Gamma(a)$ is the gamma function and $\gamma(a, b)$ is the lower incomplete gamma function. In particular,

$$E\{\exp(t|\log X|)\} \leq \frac{b^{-t}\Gamma(a-t) + b^t\Gamma(a+t)}{\Gamma(a)}. \quad (\text{A.16})$$

for $0 < t < a$. In our setting, $X = Q_k^-/m \sim \Gamma(m/2, \tilde{c}_1\delta/m)$ or $X = Q_k^+/m \sim \Gamma(m/2, \tilde{c}_2M_0/m)$, respectively. To derive the asymptotic order of $E[\exp\{\lambda \|\widehat{H}(f)\|_\infty\}]$ for $p/n \rightarrow c \in (0, \infty]$, where $\lambda > 0$, we first establish the asymptotic order of the ratio $\Gamma(a+t)/\Gamma(a)$ for $a \rightarrow \infty$. We distinguish the two cases where t is independent of a and where t linearly depends on a . Based on Stirling's approximation, one derives for $a > 1$ and $t > 0$

$$\begin{aligned} \frac{\Gamma(a+t)}{\Gamma(a)} &= \frac{\{2\pi(a+t)^{-1}\}^{1/2} (a+t)^{a+t} \exp(-a-t) [1 + \mathcal{O}\{(a+t)^{-1}\}]}{(2\pi/a)^{1/2} a^a \exp(-a) \{1 + \mathcal{O}(a^{-1})\}} \\ &= \{a(a+t)^{-1}\}^{1/2} \{(a+t)a^{-1}\}^a (a+t)^t \exp(-t) \left[\frac{1 + \mathcal{O}\{(a+t)^{-1}\}}{1 + \mathcal{O}(a^{-1})} \right]. \end{aligned} \quad (\text{A.17})$$

Thus, for $0 < t < a$ and t independent of a , Equation (A.17) implies for $a \rightarrow \infty$

that $\Gamma(a+t)/\Gamma(a) = \mathcal{O}(a^t)$. Similarly, it can be seen that $\Gamma(a-t)/\Gamma(a) = \mathcal{O}(a^{-t})$. If $0 < t < a$ and t linearly depends on a , i.e., $t = ca$ for some constant $c \in (0, 1)$, then we get $\Gamma(a \pm t)/\Gamma(a) = \mathcal{O}\{a^{\pm t} \exp(a)\}$ for $a \rightarrow \infty$. Hence, for a fixed λ not depending on n, p and such that $0 < \lambda < m2^{-1/2}M_j^{-1}$ we get for sufficiently large n, p

$$\begin{aligned} E[\exp\{\lambda M_j |Y_k^*|\}] &= E[\exp\{\lambda M_j 2^{-1/2} |\log(Q_k/m)|\}] \\ &\leq c_3 \sum_{b \in \{\tilde{c}_1 \delta/m, \tilde{c}_2 M_0/m\}} (bm/2)^{-\lambda M_j 2^{-1/2}} + (bm/2)^{\lambda M_j 2^{-1/2}} = \mathcal{O}(1). \end{aligned}$$

If $\lambda = cm$ such that $0 < \lambda < m2^{-1/2}M_j^{-1}$, then for sufficiently large n, p

$$\begin{aligned} E[\exp\{\lambda M_j |Y_k^*|\}] &\leq c_4 \exp(m/2) \sum_{b \in \{\tilde{c}_1 \delta/m, \tilde{c}_2 M_0/m\}} (bm/2)^{-\lambda M_j 2^{-1/2}} + (bm/2)^{\lambda M_j 2^{-1/2}} \\ &= \mathcal{O}(L^m), \end{aligned}$$

for some constant $L > \exp(1/2)$. Set $K = \min_{j=1, \dots, \tilde{T}} 2^{-1/2}M_j^{-1}$ which is a constant independent of n, p . Altogether, we showed that for $0 < \lambda < Km$ and $n, p \rightarrow \infty$

$$E[\exp\{\lambda \|\widehat{H}(f)\|_\infty\}] = \mathcal{O}(T), \quad \text{if } \lambda \text{ does not depend on } n, p, \quad (\text{A.18})$$

$$E[\exp\{\lambda \|\widehat{H}(f)\|_\infty\}] = \mathcal{O}(TL^m), \quad \text{if } \lambda = cm \text{ for } c \in (0, K). \quad (\text{A.19})$$

Bounding the right hand side of (A.15)

Noting that $\|f\|_\infty \leq M_0$ and $m/2 \exp\{\phi(-m/2)\} \in [1, 4]$ for $m \geq 1$, (A.18) implies for some constants $c_0, c_1 > 0$ and $n, p \rightarrow \infty$

$$\begin{aligned} E\|\widehat{f} - f\|_\infty^4 &\leq c_0 E\|\widehat{f}\|_\infty^4 + c_1 = c_0 E\|(m/2) \exp\{2^{1/2}\widehat{H}(f) - \phi(m/2)\}\|_\infty^4 + c_1 \\ &\leq c_0 \|(m/2)^4 \exp\{-4\phi(m/2)\}\} \cdot E[\exp\{4 \cdot 2^{1/2}\|\widehat{H}(f)\|_\infty\}] + c_1 = \mathcal{O}(T). \end{aligned}$$

Since g lies between $\widehat{H}(f)$ and $H(f)$, and $H^{-1} \propto \exp$, it follows $H^{-1}(g) \leq H^{-1}\{\widehat{H}(f)\} + f$ almost surely pointwise. Thus, for $C > \|f\|_\infty = M_0$, it holds

$$\text{pr}\{\|H^{-1}(g)\|_\infty > C\} \leq \text{pr}\left[\|H^{-1}\{\widehat{H}(f)\}\|_\infty > C - M_0\right] \leq \text{pr}\left[\|\widehat{H}(f)\|_\infty > c_1\right],$$

where $c_1 = H(C - M_0)$. Applying Markov's inequality for $t = cm$ with $c \in (0, K)$

and $C = 2L^{4/c} + M_0$, where c, K, L are the constants in (A.19), gives

$$\text{pr}\{\|H^{-1}(g)\|_\infty > C\} \leq \exp(-c_1 t) E[\exp\{t\|\widehat{H}(f)\|_\infty\}] = \mathcal{O}(TL^{-m}).$$

Thus, the right-hand side of (A.15) is asymptotically negligible to the first term in (A.15). Together with Proposition 1 it follows

$$E\|\hat{f} - f\|_\infty^2 = \mathcal{O}\{\log(np)/(nph)\} + \mathcal{O}(h^{2\beta}).$$

□

A.3.3 An upper bound on $E\|\widehat{\Sigma} - \Sigma\|^2$

Using the fact that the spectral norm of a Toeplitz matrix is upper bounded by the supremum norm of its spectral density, and that Proposition 2 holds for every $f \in \mathcal{F}_\beta$, we get

$$\sup_{f \in \mathcal{F}_\beta} E_f \|\widehat{\Sigma} - \Sigma(f)\|^2 \leq \sup_{f \in \mathcal{F}_\beta} E_f \|\hat{f} - f\|_\infty^2 = \mathcal{O}\{\log(np)/(nph)\} + \mathcal{O}(h^{2\beta}). \quad (\text{A.20})$$

A.3.4 An upper bound on $E\|\widehat{\Omega} - \Sigma^{-1}\|^2$

According to the mean value theorem, for a function g between $\widehat{H}(f)$ and $H(f)$, it holds that

$$\begin{aligned} E\|\widehat{\Omega} - \Omega\|^2 &\leq E\|1/\hat{f} - 1/f\|_\infty^2 = E\|1/H^{-1}\{\widehat{H}(f)\} - 1/H^{-1}\{H(f)\}\|_\infty^2 \\ &= E\|(1/H^{-1})'(g)\{\widehat{H}(f) - H(f)\}\|_\infty^2 \lesssim E\|1/H^{-1}(g)\{\widehat{H}(f) - H(f)\}\|_\infty^2. \end{aligned}$$

Application of the Cauchy-Schwarz inequality with a constant $C > 0$ yields

$$E\|1/\hat{f} - 1/f\|_\infty^2 \leq C^2 E\|\widehat{H}(f) - H(f)\|_\infty^2 + (E\|1/\hat{f} - 1/f\|_\infty^4)^{1/2} \text{pr} [\|1/\{H^{-1}(g)\}\|_\infty > C]^{1/2}.$$

Note that $\|1/H^{-1}(g)\|_\infty \leq 2/m \exp(2^{1/2}\|g\|_\infty) \exp\{\phi(m/2)\} \leq c_1 \|H^{-1}(g)\|_\infty$ for some constant $c_1 > 0$ not depending on n, p . Choosing the same constant C as in the proof of Proposition 2 it follows

$$\text{pr} [\|1/\{H^{-1}(g)\}\|_\infty > C] = \mathcal{O}(TL^{-m}).$$

Noting that $\|1/f\|_\infty \leq 1/\delta$ and $2/m \exp\{\phi(m/2)\} \in [0.25, 1]$ for $m \geq 1$, (A.18) implies for some constants $c_2, c_3 > 0$ and $n, p \rightarrow \infty$

$$\begin{aligned} E\|1/\hat{f} - 1/f\|_\infty^4 &\leq c_2|(2/m)^4 \exp\{4\phi(m/2)\}| \cdot E\|\exp\{-42^{1/2}\widehat{H}(f)\}\|_\infty + c_3 \\ &\leq c_2|(2/m)^4 \exp\{4\phi(m/2)\}| \cdot E\exp\{42^{1/2}\|\widehat{H}(f)\|_\infty\} + c_3 = \mathcal{O}(T). \end{aligned}$$

Since the derived bounds hold for each $\Sigma(f)$ with $f \in \mathcal{F}_\beta$, we get all together

$$\sup_{f \in \mathcal{F}_\beta} E_f[\|\widehat{\Omega} - \Sigma^{-1}(f)\|^2] = \mathcal{O}\{\log(np)/(nph)\} + \mathcal{O}(h^{2\beta}). \quad (\text{A.21})$$

A.3.5 Optimal bandwidth parameter h

Minimizing the right side of (A.20) for the bandwidth parameter h yields $h \asymp \{\log(np)/(np)\}^{\frac{1}{2\beta+1}}$. In particular, $h \rightarrow 0$. Furthermore,

$$hT \geq cp^{1-\min\{\beta,1\}/3-(1+\min\{1,\beta\})/(2\beta+1)}\{\log(np)\}^{1/(2\beta+1)} \rightarrow \infty$$

since by assumption $n \lesssim p^{\min\{1,\beta\}}$ and $T = \lfloor p^v \rfloor$ with $v \in (1 - \min\{1, \beta\}/3, 1)$. Thus, substituting $h \asymp \{\log(np)/(np)\}^{1/(2\beta+1)}$ into (A.20) gives the second result. \square

B Proofs of Auxiliary Lemmas for Theorem 1

This section states three technical lemmas needed for the proof of Theorem 1. The first lemma lists some properties of the kernel K_h and its extension \mathcal{K}_h on the real line. The proof is based on Schwarz and Krivobokova (2016) and (Schwarz, 2012).

Lemma 2. *Let $h > 0$ be the bandwidth parameter depending on N .*

(i) *There are constants $0 < C < \infty$ and $0 < \gamma < 1$ such that for all $x, t \in [0, 1]$*

$$\begin{aligned} |\mathcal{K}_h(x, t)| &< C\gamma^{|x-t|/h}, \\ |K_h(x, t)| &< C[\gamma^{|x-t|/h} + \gamma^{1/h}\{\gamma^{(x-t)/h} + \gamma^{(t-x)/h}\}/(1 - \gamma^{1/h})]. \end{aligned}$$

(ii) Let $t_i = (i - 1)/(N - 1)$, $i = 1, \dots, N$. If $Nh \rightarrow \infty$ for $N \rightarrow \infty$, then

$$\frac{1}{Nh} \sum_{i=1}^N \gamma_h(x, t_i) = \mathcal{O}(1), \quad \frac{1}{Nh} \sum_{i=1}^N \gamma_h^2(x, t_i) = \mathcal{O}(1)$$

uniformly for $x \in [0, 1]$, where $\gamma_h(x) = \gamma^{|x-t|/h} + \gamma^{1/h} \{ \gamma^{(x-t)/h} + \gamma^{(t-x)/h} \} / (1 - \gamma^{1/h})$.

(iii) It holds

$$\begin{aligned} h^{-1} \int_{-\infty}^{\infty} (x-t)^m \mathcal{K}_h(x, t) dt &= \delta_{m,0}, & \text{for } m = 0, \dots, 2q-1, \\ h^{-1} \int_{-\infty}^{\infty} (x-t)^m \mathcal{K}_h(x, t) dt &\neq 0, & \text{for } m = 2q. \end{aligned}$$

Proof. (i) See Lemma 16 of Schwarz (2012) for the proof of the first statement. Furthermore, for $x, t \in [0, 1]$ holds

$$\begin{aligned} |K_h(x, t)| &\leq \sum_{l=-\infty}^{\infty} |\mathcal{K}_h(x, t+l)| \\ &\leq C \sum_{l=-\infty}^{\infty} \gamma^{|x-t-l|/h} = C \left\{ \gamma^{|x-t|/h} + \sum_{l>0} \gamma^{(x-t+l)/h} + \sum_{l>0} \gamma^{(-x+t+l)/h} \right\} \\ &= C [\gamma^{|x-t|/h} + \gamma^{1/h} \{ \gamma^{(x-t)/h} + \gamma^{(t-x)/h} \} / (1 - \gamma^{1/h})]. \end{aligned}$$

(ii) Since $\gamma_h(x, \cdot)$ is differentiable everywhere except at x , it holds

$$\begin{aligned} \frac{1}{Nh} \sum_{i=1}^N \gamma_h(x, t_i) &= h^{-1} \int_0^1 \gamma_h(x, t) dt + \mathcal{O}\{(Nh)^{-1}\} \\ &= h^{-1} \int_0^1 \gamma^{|x-t|/h} dt + h^{-1} \frac{\gamma^{1/h}}{1 - \gamma^{1/h}} \int_0^1 \gamma^{(x-t)/h} + \gamma^{(t-x)/h} dt + \mathcal{O}\{(Nh)^{-1}\}. \end{aligned}$$

Note that

$$\begin{aligned} h^{-1} \int_0^1 \gamma^{|x-t|/h} dt &= \{ \gamma^{(1-x)/h} + \gamma^{x/h} - 2 \} / \log \gamma \\ \text{and } h^{-1} \int_0^1 \gamma^{(x-t)/h} + \gamma^{(t-x)/h} dx &= \gamma^{-t/h} \{ \gamma^{1/h} - 1 \} / \log \gamma - \gamma^{t/h} \{ \gamma^{-1/h} - 1 \} / \log \gamma. \end{aligned}$$

In particular, for some constants $C_1, C_2 > 0$ depending on $\gamma \in (0, 1)$ but not on h and x , it holds $h^{-1} \int_0^1 \gamma^{|x-t|/h} dt \leq C_1$ and $h^{-1} \gamma^{1/h} (1 - \gamma^{1/h})^{-1} \int_0^1 \gamma^{(x-t)/h} + \gamma^{(t-x)/h} dx \leq C_2$.

C_2 . The proof to show $h^{-1} \int_0^1 \gamma_h(x, t)^2 dt \leq C_3$ for some constant $C_3 > 0$ is similar. By assumption $(Nh)^{-1} = o(1)$ for $N \rightarrow \infty$ which concludes the proof.

(iii) See Lemma 15 of Schwarz (2012) with $p = 2q - 1$. □

The next lemma below states that the sum of the correlated gamma random variables in each bin can be rewritten as a sum of independent gamma random variables.

Lemma 3. *Let $\Sigma = \Sigma(f)$ with $f \in \mathcal{F}_\beta$ and $\beta > 0$. Then, for $n, p \rightarrow \infty$ such that $p/n \rightarrow c \in (0, \infty]$ and for $p \rightarrow \infty$ and n constant, $Q_k = \sum_{j=(k-1)p/T+1}^{kp/T} \sum_{i=1}^n \tilde{W}_{i,j}$ ($k = 1, \dots, T$) where*

$$\tilde{W}_{i,j} \stackrel{\text{indep.}}{\sim} \Gamma \left\{ 1/2, 2f(x_j) + \mathcal{O} \left(T^{-1} + T^{-1} p^{1-\beta} \log p \right) \right\}$$

for $i = 1, \dots, n$ and $j = (k-1)m+1, \dots, km$, and $x_j = (j-1)/(2p-2)$.

Proof. It is sufficient to show the statement for $n = 1$ by independence of the Y_i . Then, the number of points per bin is $m = p/T$. For simplicity, the index i is skipped in the following. First, we write Q_k as a matrix-vector product and refactor it so that it corresponds to a sum of independent scaled chi-squared random variables. In the second step, we calculate the scaling factors. Let $E^{(km)}$ be a diagonal matrix with ones on the $(k-1)m+1, \dots, km$ th entries and otherwise zero diagonal elements. Then,

$$Q_k = \sum_{j=(k-1)m+1}^{km} W_j = Y^T D E^{(km)} D Y.$$

Define $X = \Sigma^{-1/2} Y \sim \mathcal{N}_p(0_p, I_p)$, where I_p is the $p \times p$ identity matrix. Let $U^T \Gamma U$ be the eigendecomposition of $\Sigma^{1/2} D E^{(km)} D \Sigma^{1/2}$ with eigenvalues $(\lambda_j)_{j=1}^p$. The matrix $\Sigma^{1/2}$ is invertible since Σ invertible. Then,

$$Q_k = X^T \Sigma^{1/2} D E^{(km)} D \Sigma^{1/2} X = X^T U^T \Gamma U X = \tilde{X}^T \Gamma \tilde{X} = \sum_{j=1}^p \lambda_j \tilde{X}_j^2,$$

where $\tilde{X} = UX$. Since U is an orthogonal matrix, it follows that $\tilde{X} \sim \mathcal{N}_p(0_p, I_p)$. In particular, Q_k is a sum of independent scaled chi-squared random variables $\tilde{W}_j = \lambda_j \tilde{X}_j^2 \sim \Gamma(1/2, 2\lambda_j)$, where the scaling factors are the eigenvalues λ_j . It remains to

calculate the λ_j . For this we use that the matrix $\Sigma^{1/2}DE^{(km)}D\Sigma^{1/2}$ is similar to the matrix

$$A = D\Sigma^{-1/2}(\Sigma^{1/2}DE^{(km)}D\Sigma^{1/2})\Sigma^{1/2}D = E^{(km)}D\Sigma D.$$

In particular, $\Sigma^{1/2}DE^{(km)}D\Sigma^{1/2}$ has the same eigenvalues as A . The rows of A are zero except for the $(k-1)m+1, \dots, km$ th rows, which equal the $(k-1)m+1, \dots, km$ th rows of $D\Sigma D$. By Lemma 1,

$$(D\Sigma D)_{i,j} = f(x_i)\delta_{i,j} + \frac{1 + (-1)^{|i-j|}}{2} \mathcal{O}(p^{-1} + p^{-\beta} \log p).$$

Define $B = (E^{(km)}D\Sigma DE^{(km)})_{r,s=(k-1)m+1}^{km}$. Then, $\lambda(A) = \lambda(B) \cup \{0\}$ and A has an eigenvalue zero with multiplicity at least $p-m$. Since B is symmetric all eigenvalues are real-valued. Application of the Gershgorin circle theorem to B yields that the remaining m eigenvalues $\lambda_{(k-1)m+1}, \dots, \lambda_{km}$ are contained in the following set

$$\bigcup_{j=(k-1)m+1}^{km} \left\{ z \in \mathbb{R} : |f(x_j) + \mathcal{O}(p^{-1} + p^{-\beta} \log p) - z| = \mathcal{O}(mp^{-1} + mp^{-\beta} \log p) \right\}.$$

Since f is $\min\{\beta, 1\}$ -Hölder continuous, we have $\lambda_j = f(x_j) + \mathcal{O}(mp^{-1} + mp^{-\beta} \log p)$, for $j = (k-1)m+1, \dots, km$. The proof is concluded using $T^{-1} = mp^{-1}$. \square

Finally, Lemma 4 gives explicit bounds for the stochastic and deterministic errors of the variance-stabilizing transform.

Lemma 4. *If $\Sigma = \Sigma(f)$ with $f \in \mathcal{F}_\beta$ and $\beta > 0$, then $Y_k^* = 2^{-1/2} \log(Q_k/m)$ can be written as*

$$Y_k^* = H \{f(x_k)\} + \epsilon_k + m^{-1/2} Z_k + \xi_k, \quad (k = 1, \dots, T)$$

where $x_k = (k-1)/(2T-2)$, $|\epsilon_k| \lesssim (np)^{-1} + (np)^{-\beta} \log p$, $Z_k \sim \mathcal{N}(0, 1)$, and $E(\xi_k) = 0$. Furthermore,

$$\begin{aligned} E|\xi_k|^\ell &\lesssim (\log m)^{2\ell} \left\{ m^{-\ell} + (T^{-1} + T^{-1}p^{1-\beta} \log p)^\ell \right\} & (\ell \in \mathbb{N}_{>1}), \\ \text{cov}(Z_k, Z_l) &= \mathcal{O}\{mp^{-2} + mp^{-2\beta}(\log p)^2\} & (k \neq l = 1, \dots, T). \end{aligned}$$

The results hold for $n, p \rightarrow \infty$ such that $p/n \rightarrow c \in (0, \infty]$ and for $p \rightarrow \infty$ with n constant.

Proof. In the regression setting of Cai and Zhou (2010) and Brown et al. (2010) the gamma random variables in each bin are independent. Using Lemma 3, we can rewrite our setting into one with independent observations per bin. Thus, the first step of the proof is to apply the results of Cai and Zhou (2010) and Brown et al. (2010) on the approximation of Y_k^* by a Gaussian random variable $m^{-1/2}Z_k$ and a non-Gaussian remainder ξ_k . Since in our setting the observations of different bins $i \neq j$ are correlated, the covariance between the Gaussian random variables is derived in the second part of the proof.

By Lemma 3, Q_k can be written as sum of $m = np/T$ independent gamma random variables with mean function $\tilde{f}(x) = f(x) + S(x)$, where $S(x) = \mathcal{O}(T^{-1} + T^{-1}p^{1-\beta} \log p)$. It follows from Lemma 1 and 3 that the S term depends continuously on $x \in [0, 1]$ and that a global constant hidden in the \mathcal{O} term exists which is independent of the x . Furthermore, $f \in [\delta, M_0] \subset \mathbb{R}_{>0}$ by assumption. As \tilde{f} is the mean of gamma random variables, it holds that $\tilde{f} > 0$. Thus, \tilde{f} is continuous and takes values in a compact set $[\epsilon, \nu] \subset \mathbb{R}_{>0}$ of the support of the gamma distribution. By Theorem 1 of Cai and Zhou (2010) for the gamma distribution it follows

$$Y_k^* = H \left\{ \tilde{f}(x_k^*) \right\} + m^{-1/2}Z_k + \xi_k \quad (k = 1, \dots, T),$$

where $(k-1)/(2T-2) \leq x_k^* \leq k/(2T-2)$, $Z_k \sim \mathcal{N}(0, 1)$, and ξ_k is a mean zero random variable. Z_k is defined via quantile coupling. It is the Gaussian approximation to the standardized version of Q_k where the W_{ij} in the k th bin are assumed to be i.i.d. In particular, Z_k approximates

$$\bar{Q}_k = \frac{\sum_{j=(k-1)p/T+1}^{kp/T} \sum_{i=1}^n \bar{W}_{i,j} - m\tilde{f}(x_k^*)}{(2m)^{1/2}\tilde{f}(x_k^*)},$$

where $\bar{W}_{i,j} \stackrel{\text{i.i.d.}}{\sim} \Gamma(1/2, 2\tilde{f}(x_k^*))$ and such that $\text{cov}(\bar{W}_{i,j}, \bar{W}_{i,h}) = \text{cov}(W_{i,j}, W_{i,h})$ for $j = (k-1)p/T + 1, \dots, kp/T$ and $h \in \{1, \dots, p\} \setminus \{(k-1)p/T + 1, \dots, kp/T\}$.

Let θ be the maximum difference of the observations' means in each bin. Then,

$$\theta = \max_{k=1, \dots, T} \max_{j, l=(k-1)p/T+1, \dots, kp/T} \left| E[\tilde{W}_{1,j}] - E[\tilde{W}_{1,l}] \right| \leq c_1 (T^{-1} + T^{-1}p^{1-\beta} \log p).$$

Application of Lemma 4 and Theorem 1 of Brown et al. (2010) yield that ξ_k satisfies

$$E[|\xi_k|^\ell] \lesssim (\log m)^{2\ell} \{m^{-\ell} + (T^{-1} + T^{-1}p^{1-\beta} \log p)^\ell\}$$

for any constant integer $\ell > 0$ and where the hidden constant depends on ℓ . Next,

$$Y_k^* = H \left\{ f \left(\frac{k-1}{2T-2} \right) \right\} + \epsilon_k + m^{-1/2} Z_k + \xi_k \quad (k = 1, \dots, T),$$

where $\epsilon_k = H[f\{(k-1)/(2T-2)\}] - H\{\tilde{f}(x_k^*)\}$ and $|\epsilon_k| \lesssim (np)^{-1} + (np)^{-\beta} \log p$ by the Lipschitz continuity of the logarithm and the α -Hölder continuity of f .

To compute $\text{cov}(Z_k, Z_l)$ for $k \neq l$ we use Hoeffding's covariance identity. In particular, we show that $\text{cov}(Z_k, Z_l) \lesssim \text{cov}(\bar{Q}_k, \bar{Q}_l)$. The claim then follows from

$$0 \leq \text{cov}(\bar{Q}_k, \bar{Q}_l) = \frac{m \mathcal{O}\{\text{cov}(W_{i,j}, W_{i,h})\}}{2\tilde{f}(x_k^*)\tilde{f}(x_l^*)} = \mathcal{O}(mp^{-2} + mp^{-2\beta} \log p),$$

where $j = (k-1)p/T + 1, \dots, kp/T$ and $h = (l-1)p/T + 1, \dots, lp/T$.

Let Φ and $F_{\bar{Q}}$ denote the cumulative distribution functions of Z_k, Z_l, \bar{Q}_k and \bar{Q}_l . Since the Z_k are defined via quantile coupling, it holds $Z_k = \Phi^{-1}\{F_{\bar{Q}}(\bar{Q}_k)\}$, see Komlós et al. (1975); Mason and Zhou (2012). Furthermore, define the uniform random variables $U_k = \Phi(Z_k) = F_{\bar{Q}}(\bar{Q}_k)$ and $U_l = \Phi(Z_l) = F_{\bar{Q}}(\bar{Q}_l)$ with cumulative distribution function F_U . The corresponding joint cumulative distribution functions are denoted by $F_{Z,Z}, F_{\bar{Q},\bar{Q}}, F_{U,U}$. By Hoeffding's covariance identity,

$$\begin{aligned} \text{cov}(\bar{Q}_k, \bar{Q}_l) &= \int_{\mathbb{R}} \int_{\mathbb{R}} F_{\bar{Q},\bar{Q}}(q, r) - F_{\bar{Q}}(q)F_{\bar{Q}}(r) \, dq \, dr \\ &= \int_{\mathbb{R}} \int_{\mathbb{R}} \{F_{Z,Z}(x, y) - \Phi(x)\Phi(y)\} \frac{\phi(x)}{f_{\bar{Q}}\{F_{\bar{Q}}^{-1}(x)\}} \frac{\phi(y)}{f_{\bar{Q}}\{F_{\bar{Q}}^{-1}(y)\}} \, dx \, dy. \end{aligned}$$

Let $\rho = \text{cov}(Z_k, Z_l)$. Then, the identity

$$F_{ZZ}(x, y) = \frac{1}{2\pi} \int_0^\rho \frac{1}{(1-r^2)^{1/2}} \exp\left\{-\frac{x^2 - 2rxy + y^2}{2(1-r^2)}\right\} \, dr + \Phi(x)\Phi(y)$$

implies $F_{Z,Z}(x, y) - \Phi(x)\Phi(y) \geq 0$ for all $x, y \in \mathbb{R}$ if and only if $\rho \geq 0$, see Equation 9.3.1.3 of Patel and Read (1996). Since $\text{cov}(\bar{Q}_k, \bar{Q}_l) \geq 0$ and the ratio of two

densities is non-negative, it follows $\text{cov}(Z_k, Z_l) \geq 0$. Furthermore,

$$\begin{aligned}
\text{cov}(Z_l, Z_k) &= \int_{\mathbb{R}} \int_{\mathbb{R}} F_{Z,Z}(x, y) - \Phi(x)\Phi(y) \, dx \, dy \\
&= \int_0^1 \int_0^1 \{F_{UU}(u, v) - F_U(u)F_U(v)\} \frac{1}{\phi\{\Phi^{-1}(u)\}} \frac{1}{\phi\{\Phi^{-1}(v)\}} \, du \, dv \\
&\leq \int_{1/2}^1 \int_{1/2}^1 \{F_{UU}(u, v) - F_U(u)F_U(v)\} \frac{1}{\phi\{\Phi^{-1}(u)\}} \frac{1}{\phi\{\Phi^{-1}(v)\}} \, du \, dv \\
&\quad + \int_0^1 \int_0^{1/2} \{F_{UU}(u, v) - F_U(u)F_U(v)\} \frac{2}{\phi\{\Phi^{-1}(u)\}} \frac{1}{\phi\{\Phi^{-1}(v)\}} \, du \, dv.
\end{aligned}$$

The last integral corresponds to $E(Z_k Z_l^-) = \text{cov}(Z_k, Z_l)/2$ where $Z_l^- = Z_l \mathbb{1}\{Z_l \leq 0\}$. It remains to show that it exists a $c > 0$ such that $f_{\bar{Q}}\{F_{\bar{Q}}^{-1}(u)\}/\phi\{\Phi^{-1}(u)\} \leq c$ for all $u \in (1/2, 1)$. Then, it follows

$$\begin{aligned}
\text{cov}(Z_l, Z_k) &\leq 2c^2 \int_0^1 \int_0^1 \{F_{UU}(u, v) - F_U(u)F_U(v)\} \frac{1}{f_{\bar{Q}}\{F_{\bar{Q}}^{-1}(u)\}} \frac{1}{f_{\bar{Q}}\{F_{\bar{Q}}^{-1}(v)\}} \, du \, dv \\
&= 2c^2 \text{cov}(\bar{Q}_k, \bar{Q}_l).
\end{aligned}$$

Furthermore, for $u \in (1/2, 1)$ we have

$$\frac{\partial}{\partial u} \frac{f_{\bar{Q}}\{F_{\bar{Q}}^{-1}(u)\}}{\phi\{\Phi^{-1}(u)\}} = \frac{f'_{\bar{Q}}\{F_{\bar{Q}}^{-1}(u)\}}{f_{\bar{Q}}\{F_{\bar{Q}}^{-1}(u)\}\phi\{\Phi^{-1}(u)\}} - \frac{\Phi^{-1}(u)f_{\bar{Q}}\{F_{\bar{Q}}^{-1}(u)\}}{\phi\{\Phi^{-1}(u)\}^2}. \quad (\text{B.1})$$

Since $\Phi^{-1}(u) > 0$ for $u \in (1/2, 1)$, the second term is positive. To see that the first term is negative for $u \in (1/2, 1)$ we rewrite $f_{\bar{Q}}$ and $F_{\bar{Q}}^{-1}$ with respect to the non-normalized gamma random variable $X = \sum_{j=(k-1)p/T+1}^{kp/T} \sum_{i=1}^n \bar{W}_{i,j} \sim \Gamma(m/2, 2\tilde{f}(x_k^*))$. Hence,

$$f_{\bar{Q}}(x) = \sigma f_X(x\sigma + \mu), \quad F_{\bar{Q}}^{-1}(u) = \sigma^{-1}\{F_X^{-1}(u) - \mu\},$$

where σ and μ are the standard deviation and the mean of X . Since the mode of $A \sim \Gamma(a, b)$ is at $b(a-1)$ and $x\sigma + \mu = 2\tilde{f}(x_k)(m/2 - 1)$ implies $x = -(2/m)^{1/2}$, it follows that $f_{\bar{Q}}(x)$ is monotone decreasing for $x \geq -(2/m)^{1/2}$. Furthermore, $F_{\bar{Q}}(- (m/2)^{1/2}) \leq 0.5$ for all $m \in \mathbb{N}$ as $f_{\bar{Q}}(x)$ is right-skewed. In particular, $- (m/2)^{1/2} \leq F_{\bar{Q}}^{-1}(1/2)$ for all $m \in \mathbb{N}$. Finally, since $f_{\bar{Q}}(- (2/m)^{1/2}) \rightarrow \phi(0)$ for

$m \rightarrow \infty$ there is a constant $c > 0$ not depending on m such that

$$\frac{f_{\bar{Q}}\{F_{\bar{Q}}^{-1}(u)\}}{\phi\{\Phi^{-1}(u)\}} \leq \frac{f_{\bar{Q}}\{-(2/m)^{1/2}\}}{\phi(0)} \leq c.$$

□

C Supplementary Material

C.1 Simulation Study with Gamma Distribution

C.1.1 Data simulation

The observations follow a centered gamma distribution with covariance matrices $\Sigma_1, \Sigma_2, \Sigma_3$ of examples 1, 2, 3, i.e., $Y_i = \Sigma_j^{1/2} Z_i$ ($j = 1, 3; i = 1, \dots, n$), where $Z_i = (z_{i,1}, \dots, z_{i,p})^T$ with $z_{i,1} + 2^{1/2}, \dots, z_{i,p} + 2^{1/2} \stackrel{\text{i.i.d.}}{\sim} \Gamma(2, 2^{-1/2})$. For example 2, the parameter `innov` of the R function `arima.sim` is used to pass the innovations $z_{i,1} + 2^{1/2}, \dots, z_{i,p} + 2^{1/2} \stackrel{\text{i.i.d.}}{\sim} \Gamma(2, 2^{-1/2})$. The resulting process is multiplied by $(1.2)^{1/2}$.

C.1.2 Derivation of the variance-stabilizing transform function

The covariance of DY_i is $\text{cov}(DY_i) = D\Sigma D$ and the marginal distribution of $D_j^T Y_i$ follows a centered gamma distribution with variance $f(x_j) + o(1)$. Thus, $D_j^T Y_i + E(D_j^T Y_i) \sim \Gamma(2, \theta)$ with $\theta = [\{f(\pi x_j) + o(1)\}/2]^{1/2}$. Recall that the density of $A \sim \Gamma(k, \theta)$ and its centered version $B = A - E[A]$ are given by

$$g_A(x) = \frac{1}{\Gamma(k)\theta^k} x^{k-1} e^{-x/\theta} \mathbb{1}\{x \geq 0\}$$

$$g_B(x) = \frac{1}{\Gamma(k)\theta^k} (x + k\theta)^{k-1} e^{-(x+k\theta)/\theta} \mathbb{1}\{x \geq -k\theta\}.$$

It follows that the density of B^2 is then

$$\begin{aligned} g_{B^2}(x) &= \frac{g_B(x^{1/2}) + g_B(-x^{1/2})}{2x^{1/2}} \mathbb{1}\{x \geq 0\} \\ &= \frac{1}{\Gamma(k)\theta^k} \frac{(x^{1/2} + k\theta)^{k-1} e^{-(x^{1/2}+k\theta)/\theta}}{2x^{1/2}} \mathbb{1}\{x \geq 0\} \\ &\quad + \frac{1}{\Gamma(k)\theta^k} \frac{(-x^{1/2} + k\theta)^{k-1} e^{-(-x^{1/2}+k\theta)/\theta}}{2x^{1/2}} \mathbb{1}\{-(k\theta) < -x^{1/2} < 0\} \end{aligned}$$

With this density one obtains $E(B^2) = k\theta^2 =$ and $\text{var}(B^2) = c_k(k\theta)^2$ for some explicit constant c_k depending on k . Hence, $E(W_{i,j}) = E\{(D_j^T Y_i)^2\} = f(\pi x_j) + o(1)$

and $\text{var}\{(D_j^T Y_i)^2\} = 5\{f(\pi x_j) + o(1)\}^2$. The corresponding variance-stabilizing function $G : \mathbb{R} \rightarrow \mathbb{R}$ satisfies $G'(\mu) = V^{-1/2}(\mu)$, where $V(\mu)$ is the variance as a function of the mean μ . In particular, for the distribution of $W_{i,j}$ one obtains $G(\mu) = 5^{-1/2} \log(\mu)$ with $\mu = f(x_j) + o(1)$. The QQ-plots in Fig. 5 confirm the correctness of the log-transform to be the variance-stabilizing function. The transformed data Y_k^* , ($k = 1, \dots, T$) for all three examples look very similar to normally distributed random variables with homogeneous variance.

C.1.3 Results

Since the variance-stabilizing function of the $W_{i,j}$ is a scaled logarithm, our method can be applied to estimate Σ from the (centered) gamma-distributed data Y_1, \dots, Y_n . The tuning parameters of the tapering estimator and for our method are chosen the same as for the setting with Gaussian data, see Section 6. The bin number $T = 500$ was selected from the QQ-plots, see also Fig. 6 in the next section. Table 4–6 show the results for (A) $p = 5000$, $n = 1$, (B) $p = 1000$, $n = 50$ and (C) $p = 5000$, $n = 10$, respectively.

Table 4: (A) $p = 5000$, $n = 1$: Errors of the Toeplitz covariance matrix and the spectral density estimators with respect to the spectral and the L_2 norm; average computation time of the covariance estimators in seconds for one Monte Carlo sample is in the last column; all numbers multiplied with 100 except the last column

	Process (1)		Process (2)		Process (3)		time in sec
	$\ \hat{\Sigma} - \Sigma\ ^2$	$\ \hat{f} - f\ _2^2$	$\ \hat{\Sigma} - \Sigma\ ^2$	$\ \hat{f} - f\ _2^2$	$\ \hat{\Sigma} - \Sigma\ ^2$	$\ \hat{f} - f\ _2^2$	
our method (GCV)	1.181	0.434	2.285	0.609	5.182	0.884	4.238
our method (ML)	0.973	0.391	2.121	0.581	4.787	0.819	4.241
tapering (CV)	0.951	0.372	2.626	0.803	4.156	1.151	4.682
sample covariance	16750.719	3380.642	20195.498	3631.043	24828.431	3597.585	0.350
our method (GCV-oracle)	0.794	0.346	1.701	0.516	4.172	0.757	
our method (ML-oracle)	0.820	0.356	1.965	0.550	4.789	0.812	
tapering (oracle)	0.759	0.335	1.313	0.443	1.991	0.539	

Table 5: (B) $p = 1000, n = 50$: Errors of the Toeplitz covariance matrix and the spectral density estimators with respect to the spectral and the L_2 norm; average computation time of the covariance estimators in seconds for one Monte Carlo sample is in the last column; all numbers multiplied with 100 except the last column

	Process (1)		Process (2)		Process (3)		time in sec
	$\ \hat{\Sigma} - \Sigma\ ^2$	$\ \hat{f} - f\ _2^2$	$\ \hat{\Sigma} - \Sigma\ ^2$	$\ \hat{f} - f\ _2^2$	$\ \hat{\Sigma} - \Sigma\ ^2$	$\ \hat{f} - f\ _2^2$	
our method (GCV)	0.125	0.042	0.457	0.142	0.590	0.095	23.169
our method (ML)	0.106	0.038	0.525	0.151	0.736	0.106	23.093
tapering (CV)	0.122	0.040	0.497	0.154	0.410	0.087	24.444
sample covariance	80.845	57.839	103.125	61.602	126.620	60.425	0.155
our method (GCV-oracle)	0.087	0.033	0.390	0.134	0.552	0.090	
our method (ML-oracle)	0.095	0.035	0.515	0.150	0.731	0.105	
tapering (oracle)	0.074	0.032	0.371	0.137	0.307	0.068	

Table 6: (C) $p = 5000, n = 10$: Errors of the Toeplitz covariance matrix and the spectral density estimators with respect to the spectral and the L_2 norm; average computation time of the covariance estimators in seconds for one Monte Carlo sample is in the last column; all numbers multiplied with 100 except the last column

	Process (1)		Process (2)		Process (3)		time in sec
	$\ \hat{\Sigma} - \Sigma\ ^2$	$\ \hat{f} - f\ _2^2$	$\ \hat{\Sigma} - \Sigma\ ^2$	$\ \hat{f} - f\ _2^2$	$\ \hat{\Sigma} - \Sigma\ ^2$	$\ \hat{f} - f\ _2^2$	
our method (GCV)	0.138	0.042	0.386	0.129	0.626	0.099	4.347
our method (ML)	0.109	0.037	0.441	0.137	0.700	0.105	4.352
tapering (CV)	0.175	0.047	0.485	0.142	0.508	0.092	680.471
sample covariance	651.720	352.037	846.298	380.690	1061033.779	381.164	1.202
our method (GCV-oracle)	0.091	0.033	0.330	0.121	0.557	0.091	
our method (ML-oracle)	0.097	0.034	0.434	0.136	0.697	0.105	
tapering (oracle)	0.076	0.031	0.307	0.120	0.305	0.068	

C.2 Simulation Study with Uniform Distribution

C.2.1 Data simulation

The observations are generated as follows: set $Y_i = \Sigma_j^{1/2} Z_i$ ($i = 1, \dots, n; j = 1, 3$) where Σ_j is the Toeplitz covariance matrix of example j and $Z_i = (z_{i,1}, \dots, z_{i,p})^T$ with $z_{i,1}, \dots, z_{i,p} \stackrel{\text{i.i.d.}}{\sim} \text{Unif}[-3^{1/2}, 3^{1/2}]$. For example 2, the parameter `innov` of the R function `arma.sim` is used to pass the innovations $X_1, \dots, X_n \stackrel{\text{i.i.d.}}{\sim} \text{Unif}[-3^{1/2}, 3^{1/2}]$. The resulting process is multiplied by $(1.2)^{1/2}$.

C.2.2 Variance-stabilizing transform function

For this example the variance-stabilizing transform function cannot be derived explicitly. The QQ-plots in Fig. 6 indicate that the log-transform is variance-stabilizing

for $(D_j^t Y_i)^2$ for all three examples, as the transformed data Y_k^* ($k = 1, \dots, T$) with $T = 500$ look very similar to normally distributed random variables with homogeneous variance. Thus, our method can be applied to estimate Σ from the data Y_1, \dots, Y_n .

C.2.3 Results

Tables 7–9 show the results for (A) $p = 5000$, $n = 1$, (B) $p = 1000$, $n = 50$ and (C) $p = 5000$, $n = 10$, respectively. The tuning parameters of the tapering estimator and for our method are chosen the same as for the setting with Gaussian data, see Section 6.

Table 7: (A) $p = 5000$, $n = 1$: Errors of the Toeplitz covariance matrix and the spectral density estimators with respect to the spectral and the L_2 norm; average computation time of the covariance estimators in seconds for one Monte Carlo sample is in the last column; all numbers multiplied with 100 except the last column

	Process (1)		Process (2)		Process (3)		time in sec
	$\ \widehat{\Sigma} - \Sigma\ ^2$	$\ \hat{f} - f\ _2^2$	$\ \widehat{\Sigma} - \Sigma\ ^2$	$\ \hat{f} - f\ _2^2$	$\ \widehat{\Sigma} - \Sigma\ ^2$	$\ \hat{f} - f\ _2^2$	
our method (GCV)	0.737	0.230	1.952	0.488	4.010	0.616	4.282
our method (ML)	0.572	0.190	1.560	0.422	3.991	0.610	4.279
tapering (CV)	0.490	0.163	2.282	0.703	2.843	0.769	4.873
sample covariance	17131.995	3599.128	19077.308	4031.457	26960.006	3770.437	0.355
our method (GCV-oracle)	0.392	0.139	1.271	0.367	3.280	0.543	
our method (ML-oracle)	0.417	0.147	1.461	0.398	3.903	0.599	
tapering (oracle)	0.371	0.130	1.022	0.314	1.463	0.342	

Table 8: (B) $p = 1000$, $n = 50$: Errors of the Toeplitz covariance matrix and the spectral density estimators with respect to the spectral and the L_2 norm; average computation time of the covariance estimators in seconds for one Monte Carlo sample is in the last column; all numbers multiplied with 100 except the last column

	Process (1)		Process (2)		Process (3)		time in sec
	$\ \widehat{\Sigma} - \Sigma\ ^2$	$\ \hat{f} - f\ _2^2$	$\ \widehat{\Sigma} - \Sigma\ ^2$	$\ \hat{f} - f\ _2^2$	$\ \widehat{\Sigma} - \Sigma\ ^2$	$\ \hat{f} - f\ _2^2$	
our method (GCV)	0.090	0.024	0.397	0.116	0.682	0.092	31.574
our method (ML)	0.079	0.021	0.452	0.123	0.766	0.096	31.473
tapering (CV)	0.134	0.030	0.424	0.126	0.423	0.074	23.444
sample covariance	80.230	56.741	102.424	61.282	123.505	58.847	0.136
our method (GCV-oracle)	0.057	0.016	0.332	0.106	0.567	0.078	
our method (ML-oracle)	0.066	0.018	0.443	0.122	0.757	0.094	
tapering (oracle)	0.047	0.015	0.318	0.110	0.260	0.052	

Table 9: (C) $p = 5000$, $n = 10$: Errors of the Toeplitz covariance matrix and the spectral density estimators with respect to the spectral and the L_2 norm; average computation time of the covariance estimators in seconds for one Monte Carlo sample is in the last column; all numbers multiplied with 100 except the last column

	Process (1)		Process (2)		Process (3)		time in sec
	$\ \widehat{\Sigma} - \Sigma\ ^2$	$\ \widehat{f} - f\ _2^2$	$\ \widehat{\Sigma} - \Sigma\ ^2$	$\ \widehat{f} - f\ _2^2$	$\ \widehat{\Sigma} - \Sigma\ ^2$	$\ \widehat{f} - f\ _2^2$	
our method (GCV)	0.090	0.023	0.353	0.112	0.568	0.079	4.292
our method (ML)	0.074	0.019	0.412	0.119	0.635	0.085	4.285
tapering (CV)	0.127	0.025	0.437	0.124	0.427	0.066	638.830
sample covariance	662.955	365.878	824.441	379.398	1049580.980	386.305	1.205
our method (GCV-oracle)	0.060	0.016	0.314	0.105	0.478	0.070	
our method (ML-oracle)	0.066	0.017	0.408	0.118	0.626	0.085	
tapering (oracle)	0.043	0.013	0.299	0.105	0.230	0.046	

C.3 QQ-Plots

In this section, QQ-plots of the transformed data Y_k^* ($k = 1, \dots, T$) for the simulated data are shown. The QQ-plots are displayed for scenario (A) $p = 5000$, $n = 1$ as it contains fewer data points than scenario (B) and (C) and thus the largest Gaussian approximation error for the transformed data Y_k^* . Figure 4 demonstrates the impact of the bin number T on the transformed data Y_k^* for example (1) with Gaussian data Y (see simulation study in Section 6 of the main article). The plots justify the choice of $T = 500$ for the simulation study, as in this case the Y_k^* are very close to Gaussian distributed random variables. Figure 5 and 6 show the QQ-plots of Y_k^* for example 1–3 with bin number $T = 500$, where the original data Y is gamma distributed or uniform distributed, respectively. The plots look similar to the QQ-plots in Fig. 4 for the Gaussian data Y and indicate that our method to for Toeplitz covariance estimation is applicable also for these non-Gaussian data.

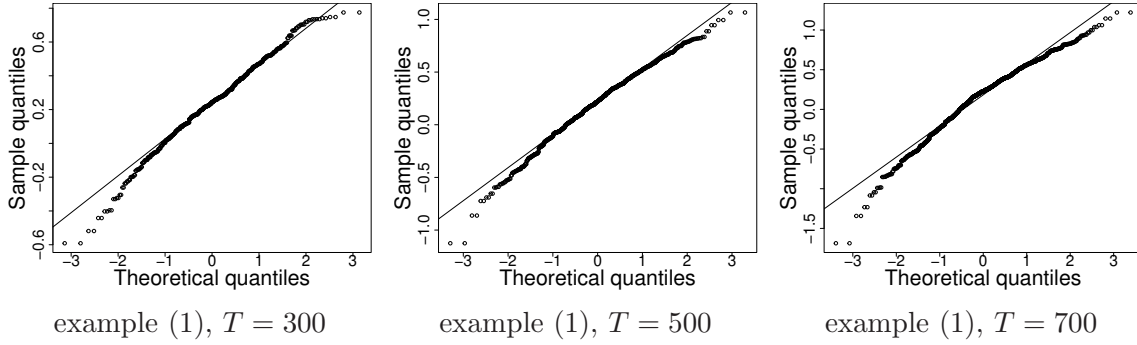


Figure 4: Simulation study with Gaussian data; QQ-plots of binned and transformed data Y_k^* ($k = 1, \dots, 2T - 2$) with different bin numbers T for example (1) with $p = 5000$, $n = 1$.

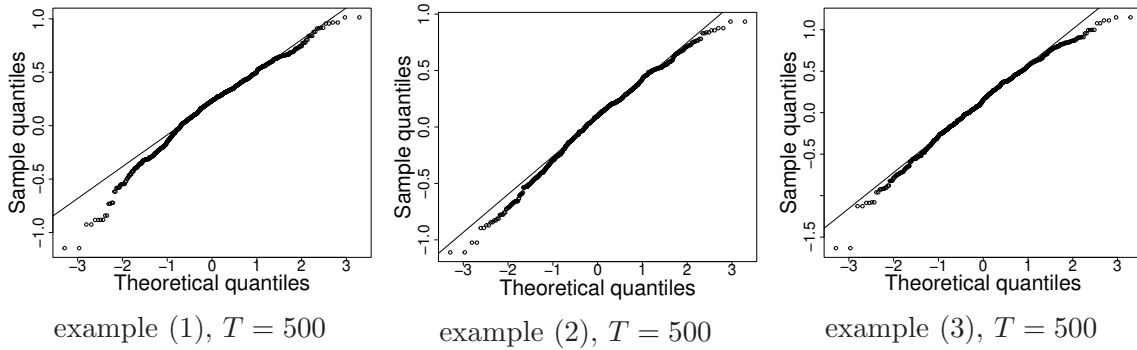


Figure 5: Simulation study with gamma data; QQ-plots of binned and transformed data Y_k^* ($k = 1, \dots, 2T - 2$) with $T = 500$ for examples (1)–(3) with $p = 5000$, $n = 1$.

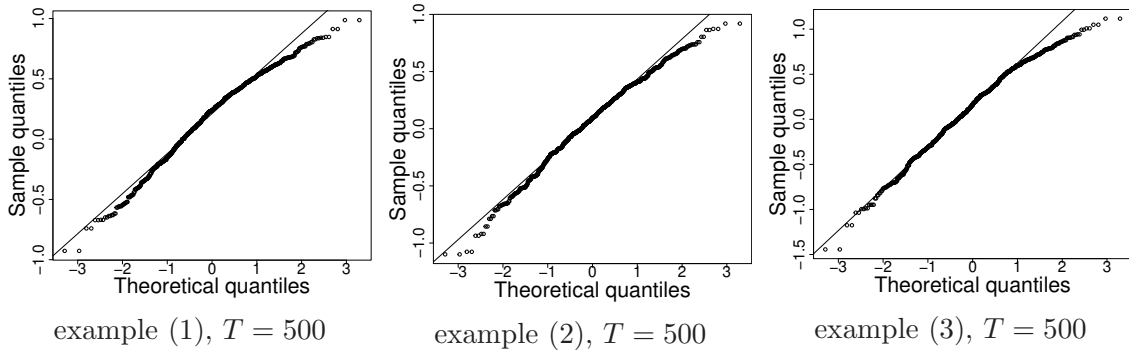


Figure 6: Simulation study with uniform data; QQ-plots of binned and transformed data Y_k^* ($k = 1, \dots, 2T - 2$) with $T = 500$ for examples (1)–(3) with $p = 5000$, $n = 1$.

References

- Abramowitz, M. and Stegun, I. A. (1964). *Handbook of mathematical functions with formulas, graphs, and mathematical tables*, volume 55. US Government printing office.
- Azuma, K. (1967). Weighted sums of certain dependent random variables. *Tohoku Mathematical Journal, Second Series*, 19(3):357–367.
- Bartlett, M. S. (1950). Periodogram analysis and continuous spectra. *Biometrika*, 37(1/2):1–16.
- Bentkus, R. (1985). Rate of uniform convergence of statistical estimators of spectral density in spaces of differentiable functions. *Lithuanian Mathematical Journal*, 25(3):209–219.
- Bickel, P. J. and Levina, E. (2008). Regularized estimation of large covariance matrices. *The Annals of Statistics*, 36(1):199–227.
- Brown, L. D., Cai, T. T., Zhou, H. H., et al. (2010). Nonparametric regression in exponential families. *The Annals of Statistics*, 38(4):2005–2046.
- Cai, T. T., Ren, Z., and Zhou, H. H. (2013). Optimal rates of convergence for estimating Toeplitz covariance matrices. *Probability Theory and Related Fields*, 156(1-2):101–143.
- Cai, T. T. and Zhou, H. H. (2010). Nonparametric regression in natural exponential families. In *Borrowing Strength: Theory Powering Applications—A Festschrift for Lawrence D. Brown*, pages 199–215. Institute of Mathematical Statistics.
- Chagny, G. (2016). An introduction to nonparametric adaptive estimation. *The Graduate Journal of Mathematics*, 1(2):105–120.
- Choudhuri, N., Ghosal, S., and Roy, A. (2004). Bayesian estimation of the spectral density of a time series. *Journal of the American Statistical Association*, 99(468):1050–1059.
- Du, X., Aubry, A., De Maio, A., and Cui, G. (2020). Toeplitz structured covariance matrix estimation for radar applications. *IEEE Signal Processing Letters*, 27:595–599.
- Edwards, M. C., Meyer, R., and Christensen, N. (2019). Bayesian nonparametric spectral density estimation using B-spline priors. *Statistics and Computing*,

- 29(1):67–78.
- Fang, Y., Wang, B., and Feng, Y. (2016). Tuning-parameter selection in regularized estimations of large covariance matrices. *Journal of Statistical Computation and Simulation*, 86(3):494–509.
- Franaszczuk, P. J., Blinowska, K. J., and Kowalczyk, M. (1985). The application of parametric multichannel spectral estimates in the study of electrical brain activity. *Biological cybernetics*, 51(4):239–247.
- Grenander, U. and Szegö, G. (1958). *Toeplitz forms and their applications*. Univ of California Press.
- Guerrero, V. M. (1993). Time-series analysis supported by power transformations. *Journal of forecasting*, 12(1):37–48.
- Hastie, T. and Tibshirani, R. (1990). *Generalized additive models*. Wiley Online Library.
- Komlós, J., Major, P., and Tusnády, G. (1975). An approximation of partial sums of independent rv'-s, and the sample df. i. *Zeitschrift für Wahrscheinlichkeitstheorie und verwandte Gebiete*, 32:111–131.
- Kooperberg, C., Stone, C. J., and Truong, Y. K. (1995). Rate of convergence for logspline spectral density estimation. *Journal of Time Series Analysis*, 16(4):389–401.
- Krivobokova, T. (2013). Smoothing parameter selection in two frameworks for penalized splines. *Journal of the Royal Statistical Society Series B: Statistical Methodology*, 75(4):725–741.
- Krivobokova, T., Briones, R., Hub, J. S., Munk, A., and de Groot, B. L. (2012). Partial least-squares functional mode analysis: application to the membrane proteins aqp1, aqy1, and clc-ec1. *Biophysical journal*, 103(4):786–796.
- Mason, D. M. and Zhou, H. H. (2012). Quantile coupling inequalities and their applications.
- Maturana-Russel, P. and Meyer, R. (2021). Bayesian spectral density estimation using p-splines with quantile-based knot placement. *Computational Statistics*, 36(3):2055–2077.
- McMurry, T. L. and Politis, D. N. (2010). Banded and tapered estimates for au-

- tocovariance matrices and the linear process bootstrap. *Journal of Time Series Analysis*, 31(6):471–482.
- Patel, J. K. and Read, C. B. (1996). *Handbook of the normal distribution*, volume 150. CRC Press.
- Pawitan, Y. and O’Sullivan, F. (1994). Nonparametric spectral density estimation using penalized Whittle likelihood. *Journal of the American Statistical Association*, 89(426):600–610.
- Pourahmadi, M. (2013). *High-dimensional covariance estimation: with high-dimensional data*, volume 882. John Wiley & Sons.
- Quah, D. (2000). Internet cluster emergence. *European economic review*, 44(4-6):1032–1044.
- Roberts, W. J. and Ephraim, Y. (2000). Hidden Markov modeling of speech using Toeplitz covariance matrices. *Speech Communication*, 31(1):1–14.
- Schoenberg, I. (1973). *Cardinal Spline Interpolation*. SIAM, Philadelphia.
- Schwarz, K. (2012). *A unified framework for spline estimators*. PhD thesis, University of Göttingen.
- Schwarz, K. and Krivobokova, T. (2016). A unified framework for spline estimators. *Biometrika*, 103(1):121–131.
- Serra, P., Krivobokova, T., et al. (2017). Adaptive empirical Bayesian smoothing splines. *Bayesian Analysis*, 12(1):219–238.
- Singer, M., Krivobokova, T., Munk, A., and De Groot, B. (2016). Partial least squares for dependent data. *Biometrika*, 103(2):351–362.
- Taqqu, M. S. and Teverovsky, V. (1997). Robustness of Whittle-type estimators for time series with long-range dependence. *Communications in statistics. Stochastic models*, 13(4):723–757.
- Thomson, D. J. (1982). Spectrum estimation and harmonic analysis. *Proceedings of the IEEE*, 70(9):1055–1096.
- Tsybakov, A. B. (2009). *Introduction to nonparametric estimation*. Springer series in statistics. Springer.
- Vershynin, R. (2018). *High-dimensional probability: An introduction with applications in data science*, volume 47. Cambridge university press.

- Wahba, G. (1980). Automatic smoothing of the log periodogram. *Journal of the American Statistical Association*, 75(369):122–132.
- Wahba, G. (1985). A comparison of GCV and GML for choosing the smoothing parameter in the generalized spline smoothing problem. *The Annals of Statistics*, 13(4).
- Walker, A. (1964). Asymptotic properties of least-squares estimates of parameters of the spectrum of a stationary non-deterministic time-series. *Journal of the Australian Mathematical Society*, 4(3):363–384.
- Welch, P. (1967). The use of fast Fourier transform for the estimation of power spectra: a method based on time averaging over short, modified periodograms. *IEEE Transactions on audio and electroacoustics*, 15(2):70–73.
- Whittle, P. (1957). Curve and periodogram smoothing. *Journal of the Royal Statistical Society: Series B (Methodological)*, 19(1):38–47.
- Wu, W. B. and Pourahmadi, M. (2009). Banding sample autocovariance matrices of stationary processes. *Statistica Sinica*, pages 1755–1768.
- Wu, W. B. and Xiao, H. (2012). Covariance matrix estimation in time series. In *Handbook of Statistics*, volume 30, pages 187–209. Elsevier.
- Zygmund, A. (2002). *Trigonometric series*, volume 1. Cambridge university press.